AD_____

Award Number: DAMD17-98-1-8286

TITLE: Glutathione Transferases and the Multidrug Resistance - Associated Protein in Prevention of Potentially Carcinogenic Oxidant Stress in Breast Cancer

PRINCIPAL INVESTIGATOR: Robin L. Haynes
Doctor Alan J. Townsend

CONTRACTING ORGANIZATION: Bowman Gray School of Medicine
Winston-Salem, North Carolina 27157

REPORT DATE: June 2001

TYPE OF REPORT: Annual Summary

PREPARED FOR: U.S. Army Medical Research and Materiel Command
Fort Detrick, Maryland 21702-5012

REPORT DOCUMENTATION PAGE

Form Approved
OMB No. 074-0188

1. AGENCY USE ONLY (Leave blank)	2. REPORT DATE	3. REPORT TYPE AND DATES COVERED
	June 2001	Annual Summary (1 Jun 98 - 31 May 01)

4. TITLE AND SUBTITLE
Glutathione Transferases and the Multidrug Resistance - Associated Protein in Prevention of Potentially Carcinogenic Oxidant Stress in Breast Cancer

5. FUNDING NUMBERS
DAMD17-98-1-8286

6. AUTHOR(S)
Robin L. Haynes
Doctor Alan J. Townsend

7. PERFORMING ORGANIZATION NAME(S) AND ADDRESS(ES)
Bowman Gray School of Medicine
Winston-Salem, North Carolina 27157
E-Mail: robin.haynes@TCH.Harvard.edu

8. PERFORMING ORGANIZATION REPORT NUMBER

9. SPONSORING / MONITORING AGENCY NAME(S) AND ADDRESS(ES)
U.S. Army Medical Research and Materiel Command
Fort Detrick, Maryland 21702-5012

10. SPONSORING / MONITORING AGENCY REPORT NUMBER

11. SUPPLEMENTARY NOTES

12a. DISTRIBUTION / AVAILABILITY STATEMENT
Approved for Public Release; Distribution Unlimited

12b. DISTRIBUTION CODE

13. ABSTRACT *(Maximum 200 Words)*

Oxidative stress has been implicated as a causative or contributory factor in breast cancer. Lipid peroxidation is one result of oxidative stress, and may be common in breast tissue due to the high fat content. A highly reactive aldehyde byproduct of lipid peroxidation, 4 hydroxy-2-nonenal (HNE) is known to damage both DNA and protein. We have determined the structural components that are most critical for HNE toxicity, using compounds analogous in structure to HNE but lacking specific structural features. With growth inhibition and apoptosis induction as endpoints, the rank order of importance was aldehyde>trans double bond>4hydroxyl. Longer lipid chains also yielded greater toxicity than shorter.

We also examined the mechanism of HNE-induced apoptosis and found that it induces stabilization and accumulation of p53 in RAW 264.7 mouse macrophage cells. However, inactivation of p53 function by expression of T-antigen showed that the apoptosis is p53-independent. The HNE-induced apoptosis was closely correlated with cytochrome c release into the cytosol. These studies indicate a link between oxidant stress-induced lipid peroxidation and apoptosis that might be important under circumstances that involve inflammation and associated oxidant stress, such as inflammatory breast cancer.

14. SUBJECT TERMS	15. NUMBER OF PAGES
Lipid peroxidation, apoptosis, hydroxynoneal, p53, mitochondria	46
	16. PRICE CODE

17. SECURITY CLASSIFICATION OF REPORT	18. SECURITY CLASSIFICATION OF THIS PAGE	19. SECURITY CLASSIFICATION OF ABSTRACT	20. LIMITATION OF ABSTRACT
Unclassified	Unclassified	Unclassified	Unlimited

Table of contents

REPORT OF INVENTIONS AND SUBCONTRACTS

(Pursuant to "Patent Rights" Contract Clause) (See Instructions on Reverse Side.)

Form Approved
OMB No. 0704-0297
Expires Jun 30, 1992

1a. NAME OF CONTRACTOR / SUBCONTRACTOR	c. CONTRACT NUMBER	2a. NAME OF GOVERNMENT PRIME CONTRACTOR	c. CONTRACT NUMBER	3. TYPE OF REPORT (X one)
Wake Forest Univ. Sch of Med	Damd17-98-1-8286	same	same	a. INTERIM ☐ b. FINAL ☐
b. ADDRESS (Include ZIP Code)	d. AWARD DATE (YYMMDD)	b. ADDRESS (Include ZIP Code)	d. AWARD DATE (YYMMDD)	4. REPORTING PERIOD (YYMMDD)
Biochemistry Dept. Medical Center Blvd, Winston-Salem, NC 27157	July 1, 1998	same	same	a. FROM b. TO

SECTION I – SUBJECT INVENTIONS

5. "SUBJECT INVENTIONS" REQUIRED TO BE REPORTED BY CONTRACTOR / SUBCONTRACTOR (If "None," so state)

a. NAME(S) OF INVENTOR(S) (Last, First, MI)	b. TITLE OF INVENTION(S)	c. DISCLOSURE NO., PATENT APPLICATION SERIAL NO. OR PATENT NO.	d. ELECTION TO FILE PATENT APPLICATIONS				e. CONFIRMATORY INSTRUMENT OR ASSIGNMENT FORWARDED TO CONTRACTING OFFICE	
			(1) United States		(2) Foreign			
			(a) Yes	(b) No	(a) Yes	(b) No	(1) Yes	(2) No
None								

f. EMPLOYER OF INVENTOR(S) NOT EMPLOYED BY CONTRACTOR / SUBCONTRACTOR		g. ELECTED FOREIGN COUNTRIES IN WHICH A PATENT APPLICATION WILL BE FILED	
(1) (a) Name of Inventor (Last, First, MI)	(2) (a) Name of Inventor (Last, First, MI)	(1) Title of Invention	(2) Foreign Countries of Patent Application
(b) Name of Employer	(b) Name of Employer		
(c) Address of Employer (Include ZIP Code)	(c) Address of Employer (Include ZIP Code)		

SECTION II – SUBCONTRACTS (Containing a "Patent Rights" clause)

6. SUBCONTRACTS AWARDED BY CONTRACTOR / SUBCONTRACTOR (If "None," so state)

a. NAME OF SUBCONTRACTOR(S)	b. ADDRESS (Include ZIP Code)	c. SUBCONTRACT NO.(S)	d. DFAR "PATENT RIGHTS"		e. DESCRIPTION OF WORK TO BE PERFORMED UNDER SUBCONTRACT(S)	f. SUBCONTRACT DATES (YYMM.	
			(1) Clause Number	(2) Date (YYMM)		(1) Award	(2) Estimated Completion
None							

SECTION III – CERTIFICATION

7. CERTIFICATION OF REPORT BY CONTRACTOR / SUBCONTRACTOR (Not required if ☐ Small Business or ☐ Non-Profit organization.) (X appropriate box)

a. NAME OF AUTHORIZED CONTRACTOR / SUBCONTRACTOR OFFICIAL (Last, First, MI)	c. I certify that the reporting party has procedures for prompt identification and timely disclosure of "Subject Inventions," that such procedures have been followed and that all "Subject Inventions" have been reported.	
Dr. Sheila Vrana		
b. TITLE	d. SIGNATURE	e. DATE SIGNED
Director of Sponsored Research	Sheila Vrana	7/3/01

DD Form 882, OCT 89 — *Previous editions are obsolete.* — 971/284

Foreword:

The original focus of this project was on the interaction between the MRP 1 multidrug resistance protein, which has activity for efflux of glutathione-conjugated molecules out of cells, and the glutathione S-transferase (GST) family of detoxifying proteins, which catalyze conjugation of carcinogens with the thiol tripeptide glutathione. Early results in this project, together with technical problems with expression of MRP 1 in transfected cell lines, led to a switch in emphasis to the mechanisms of induction of apoptosis induced by the toxic lipid peroxidation product 4-hydroxynonenal (HNE). In addition, we have examined the relative contributions of GST and aldehyde dehydrogenase families of detoxifying enzymes to prevention of cytotoxicity, macromolecular damage, and apoptosis by HNE. This work has relevance to mechanisms of oxidative stress, inflammation and carcinogenesis, as well as pathways of induction of apoptosis in breast and other forms of cancer.

This project has now been completed and Dr. Haynes received her Ph.D. in Biochemistry in Spring 2001. She began a postdoctoral fellowship at Harvard in March 2001

Introduction

Background

Oxidative stress, a subject of much recent study, causes cellular damage due to normal oxidative metabolism. It is associated with many different disease states including inflammatory diseases, aging and cancer. It has been linked to breast cancer susceptibility through the study of antioxidants such as isoflavins and vitamin E that have been shown to be anticarcinogenic agents in breast tissue. Because breast tissue has a high fat content, it is highly susceptible to oxidative damage via lipid peroxidation. The focus of this project centers on an extremely potent mediator of oxidant stress induced damage, 4-hydroxy-2-nonenal (HNE).

HNE is one of the most reactive byproducts of lipid peroxidation which results from the interaction of reactive oxygen species with cellular membranes. The data presented in the two published papers attached focuses on the contributions of individual structural components to the overall reactivity and toxicity of HNE, and on mechanisms whereby HNE induces apoptosis. This work not only contributes to knowledge about the cellular effects of HNE, but also provides evidence of a link between oxidant stress-induced lipid peroxidation and oxidant stress-induced apoptosis. The balance between oxidative damage and oxidant-induced apoptosis likely affects cancer incidence by controlling the balance between death or progression of preneoplastic cells in breast, colon, and other types of cancer.

Summary of publication # 1 (copy attached) :

Haynes, Robin L., Szweda, Luke, and Townsend, Alan J. Structure-Activity Relationships for Growth Inhibition and Induction of Apoptosis by 4-Hydroxy 2-nonenal in Raw 264.7 Cells. *Molecular Pharmacology* , **58 :** 788 – 794, 2000.

(also presented as a poster at a Keystone Conference on Apoptosis, Keystone, CO , April 1999, and again at the June 2000 Era of Hope Meeting in Atlanta).

Key findings:

1) There is a dramatic decrease in toxicity when cells are exposed to nonenoic acid which lacks the aldehyde yet retains the double bond (IC_{50} = 1770 μM) as compared to trans-2 nonenal (IC_{50} =24 μM). This decrease in toxicity is also seen with the apoptotic endpoint DNA fragmentation. The loss of the aldehyde reduces the reactivity of the double bond, and also prevents the formation of LINE-protein crosslinks.

2) When cells are treated with nonanal, a 9- carbon alkyl analog which retains the aldehyde but lacks the double bond and C4 hydroxy, an intermediate toxicity (IC_{50} =308 μM) between trans-2 nonenal ((IC_{50} = 24 μM) and nonenoic acid ((IC_{50} = I 770 μM) is seen. The loss of the aldehyde in nonenoic acid results in a 74-fold decrease in toxicity compared to trans-2-nonenal. The lack of a double bond in nonanal decreases toxicity 13-fold relative to trans-2-nonenal. The loss of the double bond prevents Michael additions at the C3 position, and also removes the potentiation of the reactivity of the aldehyde which alone can interact with proteins to form Schiff base adducts.

3) Both the aldehyde and C2=C3 double bond are essential for the full toxicity of HNE and induction of apoptosis. Their effects are additive and mutually interactive.

4) The third reactive group, the 4-hydroxy, contributes much less to the toxicity of HNE, as evidenced by the 2.7 fold decrease in the toxicity of trans-2-nonenal as compared to HNE (IC_{50} of 24 μM vs. 9 μM for HNE) and the parallel differences for induction of apoptotic DNA fragmentation for these two analogs.

5) The length of the alkenyl chain is important in the toxicity of the compound. Increasing the alkenal chain increases the toxicity, both in growth inhibition and in apoptosis induction.

6) Overexpression of human aldehyde dehydrogenase-3, which oxidizes the aldehyde of HNE into a carboxylic acid, completely protects the cells from apoptotic induction to at least 70 μM HNE. It also protects the cell against HNE-protein adduct formation. Such a strong protection supports the conclusion that the aldehyde of HNE contributes a significant potency to the overall reactivity of the compound. It also confirms that the aldehyde group is exerting its toxicity intracellularly rather than at the plasma membrane.

Summary of publication # 2 (copy attached) :

Townsend, Alan J., Leone-Kabler, Sandra, **Haynes, Robin L.**, Wu, Yinghui, Szweda, Luke and Bunting, Kevin D. Selective Protection By Stably Transfected Human ALDH3A1 (but not Human ALDH1A1) Against Toxicity of Aliphatic Aldehydes in V79 Cells. *Chem. – Biol. Interact.* **130-132:** 261 – 273, 2001.

Toxic medium chain length alkanals, alkenals, and 4-hydroxyalkenals that are generated during lipid peroxidation are potential substrates for aldehyde dehydrogenase (ALDH) isoforms. We have developed transgenic cell lines to examine the potential for either human hALDH1A1 or hALDH3A1 to protect against damage mediated by these toxic aldehydes.

Key findings:

1) Using crude cytosols from stably transfected cell lines, these aldehydes were confirmed to be excellent substrates for ALDH3A1 but were poorly oxidized by hALDH1A1.

2) Expression of hALDH3A1 by stable transfection in V79 cells conferred a high level of protection against growth inhibition by the medium-chain length aldehyde substrates with highest substrate activity, including hexanal, trans-2-hexenal, trans-2-octenal, trans-2-nonenal, and 4-hydroxy-2-nonenal (HNE).

3) This was reflected in a parallel ability of hALDH3A1 to prevent depletion of glutathione by these aldehydes.

4) Expression of hALDH3 completely blocked the potent induction of apoptosis by HNE in both V79 cells and in a RAW 264.7 murine macrophage cell line, consistent with prevention of HNE-protein adduct formation.

5) In contrast, hALDH1A1 expression provided only moderate protection against trans-2-nonenal, and none against the other 6 – 9 carbon aldehydes.

6) Neither hALDH1A1 nor hALDH3A1 conferred any protection against acrolein, acetaldehyde, or chloroacetaldehyde. A small degree of protection against malondialdehyde was afforded by hALDH1A1, but not hALDH3A1.

7) These studies demonstrate that expression of class 3 ALDH, but not class 1 ALDH, can be an important determinant of cellular resistance to toxicity mediated by aldehydes of intermediate chain length that are produced during lipid peroxidation.

Summary of publication # 3 (copy attached) :

Haynes, R. L., Brune, B., and Townsend, A. J. Apoptosis in RAW 264.7 cells exposed to 4-hydroxy-2-nonenal: dependence on cytochrome C release but not p53 accumulation. *Free Rad Biol Med* **30:** 884-894, 2001.

(also presented at the April 2000 American Assocociation for Cancer Research meeting, San Francisco, CA, and at the June 2000 Era of Hope Meeting in Atlanta).

Key findings:

1) Expression of the anti-apoptotic protein Bcl-2 in stably transfected RAW 264.7 cells prevented HNE–induced internucleosomal DNA fragmentation and apoptosis, and these cells resume growth after a temporary (24-48 hr) growth delay.

2) While parental RAW 264.7 cells released mitochondrial cytochrome c within 3 hours after HNE exposure, expression of Bcl-2 prevented cytochrome c release.

3) In control cells, p53 protein levels peaked at 6-9 hours after HNE exposure and then declined, while in Bcl-2 expressing cells, p53 levels were maximal at 6-9 hours and remained elevated up to 96 hours.

4) Expression of SV40 large T-antigen, which forms a stable complex with p53 protein, via stable transfection blocked transactivation of the p53-regulated gene $p21^{WAF1/CIP1}$, but did not affect induction of apoptosis by HNE, suggesting that p53 function is not important in HNE induced apoptosis.

These results indicate that cytochrome c release, but not p53 accumulation, plays an essential role in HNE-induced apoptosis in RAW 264.7 cells.

Summary of publication # 4 (in preparation) :

Haynes, Robin L., Morrow, Charles S., and Townsend, Alan J. Enhanced apoptosis after exposure to thiol-reactive electrophiles in transgenic cell lines expressing high levels of glutathione S-transferases. *In preparation.*

Key findings:

1) Expression of murine GSTA4 in V79 cells results in paradoxically *enhanced sensitivity* to HNE, rather than protection due to conjugation, as expected. This may yet be due to accumulation of the HNE-SG conjugate, which can tautomerize to an open-chain aldehyde that may retain significant reactivity and hence toxicity.

2) Similarly, expression of murine GSTM1 in V79 cells results in paradoxically *enhanced sensitivity* to the toxicity of the carcinogen 4-nitroquinoline-1-oxide, again rather than protection, as expected. This was *not* due to accumulation of the GSH conjugated product, again contrary to expectations.

3) The current hypothesis is that these results may reflect GSH depletion that dominates the outcome, rather than the toxicity of the parent electrophile and its detoxification by GSTs. However, result #1 may be due to continued toxicity of the conjugated product.

Reportable Outcomes

Ph.D. Degree awarded:

Dr. Robin L. Haynes received her Ph.D. degree in Biochemistry in the Spring of 2001. She has recently accepted a postdoctoral fellowship appointment at Harvard University, Boston, MA.

Abstracts: (copies attached)

1. **Haynes, R. L.** , Willingham, M., Szweda, L., and Townsend, A. J. Structure-Activity and Mechanistic Studies on Induction of Apoptosis by 4-Hydroxy-2-nonenal in RAW 264.7 Cells. *Proc. Keystone Symp. On Apoptosis, Keystone, CO , April 1999.*

2. **R. L. Haynes** and A. Townsend. Lipid Peroxidation product 4-Hydroxy 2 Nonenal induces cytochrome c dependent, p53 independent apoptosis in murine macrophage line RAW 264.7. *American Association for Cancer Research,* Conference on Cell Death. Lake Tahoe, NV. Feb. 2000.

3. **Haynes, R. L.** and Townsend, A. J. Patterns of p53 Accumulation and Cytochrome c Release Upon Induction of Apoptosis by the Lipid Peroxidation Product 4-Hydroxy-2-nonenal in RAW 264.7 cells. *Proc. Amer. Assoc. Cancer Res.* **41:** # 4137 (p. 651) , 2000.

4. **R. L. Haynes** and A. Townsend. Structure-Activity and Mechanistic Studies on the Toxicity of 4-Hydroxy 2-Nonenal, byproduct of the peroxidation of Polyunsaturated Fatty Acids. *Dept of Defense "Era of Hope" Breast Cancer Symposium.* Atlanta, Ga. June 2000.

Manuscripts:(copies of # 1 – 3 are attached)

1. **Haynes, Robin L.**, Szweda, Luke, and Townsend, Alan J. Structure-Activity Relationships for Growth Inhibition and Induction of Apoptosis by 4-Hydroxy 2-nonenal in Raw 264.7 Cells. *Molecular Pharmacology* , **58 :** 788 – 794, 2000.

2. **Haynes, R. L.**, Brune, B., and Townsend, A. J. Apoptosis in RAW 264.7 cells exposed to 4-hydroxy-2-nonenal: dependence on cytochrome C release but not p53 accumulation. *Free Rad Biol Med* **30:** 884-894, 2001.

3. Townsend, Alan J., Leone-Kabler, Sandra, **Haynes, Robin L.**, Wu, Yinghui, Szweda, Luke and Bunting, Kevin D. Selective Protection By Stably Transfected Human ALDH3A1 (but not Human ALDH1A1) Against Toxicity of Aliphatic Aldehydes in V79 Cells. *Chem. – Biol. Interact.* **130-132:** 261 – 273, 2001.

4. **Haynes, Robin L.**, Morrow, Charles S., and Townsend, Alan J. Enhanced apoptosis after exposure to thiol-reactive electrophiles in transgenic cell lines expressing high levels of glutathione S-transferases. *In preparation.*

Cell lines created:

1. Multiple clones of RAW 264.7 cells overexpressing SV40 Large T-antigen.
2. Multiple clones of RAW 264.7 cells overexpressing hALDH3.
3. Several clones of V79 cells overexpressing murine GSTA4.

Abstract #1 :

Structure-Activity and Mechanistic Studies on Induction of Apoptosis by 4-Hydroxy-2-nonenal in RAW 264.7 Cell. Robin L. Haynes, Mark Willingham, Luke Szweda, and Alan J. Townsend. Biochemistry Dept., Wake Forest Univ. School of Medicine, Winston-Salem, NC 27157

4- hydroxy-2-nonenal (HNE) is a highly reactive lipid aldehyde byproduct of the peroxidation of cellular membranes. It has been shown to induce apoptosis in certain cell lines and is thought to be a potential mediator of oxidant stress induced apoptosis. Here we present our findings regarding structural determinants and mechanistic aspects of induction of apoptosis by HNE.

In the mouse alveolar macrophage cell line RAW 264.7 apoptosis is induced in a dose dependent manner as seen by internucleasomal DNA fragmentation and caspase activation. Both indices are seen at concentrations as low as 25 - 30uM HNE. Using time lapse video microscopy, we have shown that at 50uM HNE greater than 90% of the cells have formed apoptotic blebs, blistered, and lysed by 18 hours. Structure-activity relationships have been examined to determine the importance of individual structural components of HNE in the apoptosis induction mechanism. Using congeners with various chain lengths, and with DNA laddering as an index of apoptosis, we have shown that the potency of apoptosis induction increases greatly with the length of the fatty acid chain. Nonanal, which lacks the trans 3,4-double bond, shows a decreased potency compared to analogous aldehydes. Nonenoic acid, which lacks the C1-aldehyde yet retains the double bond, shows a considerable loss of potency from that of all compounds tested including nonanal. These results are consistant with growth inhibition/cell survival data which give an IC50 of 1500uM for nonenoic acid and IC50's ranging from 10uM - 200uM for all other congeners retaining the aldehyde. The importance of the aldehyde in HNE toxicity is supported by studies in which RAW cells overexpressing the aldehyde metabolizing enzyme aldehyde dehydrogenase (ALDH) show complete protection against HNE induced apoptosis as well as HNE -protein adduct formation.

In addition to stuctural-activity correlations we are also studying mechanistic aspects of HNE induced apoptosis.Unexpectedly, there was no acute depletion of GSH up to several hours after exposure to HNE. Because HNE can damage DNA, p53 expression was measured; however no p53 protein accumulation was detected within the time and concentration range relevant to induction. An alternate mechanism of induction may involve direct effects of HNE on mitochondria. Evidence supporting the role of mitochondria in HNE induced apoptosis is seen in RAW cells overexpressing the anti-apoptotic protein BCL2. This overexpression renders cells resistant to HNE induced apoptosis suggesting that mitochondrial permeability (PT) modulation plays a role in the induction pathway. Mitochondial transmembrane potential studies using flow cytometry and the potential sensitive dye DiOC6(3) are currently underway. *Supported by NIH Grant # CA-76283, and DOD Grant # DAMD 17-98-8286.*

Poster presented to the Keystone Conference on Apoptosis, Keystone, CO, 1999.

Abstract #2 :

4-Hydroxy-2 nonenal (HNE), a highly reactive aldehyde product of the peroxidation of w- fatty acids, has been shown to induce apoptosis in certain cell lines. When RAW 264.7 murine macrophage cells were treated with HNE, apoptosis was induced in a dose dependent manner as seen by caspase activation and internucleasomal DNA fragmentation. To examine the possible involvement of HNE induced DNA damage in the apoptotic induction, p53 levels were examined. After a 1 hour treatment with 50mM HNE, p53 levels increased, peaking at 6 hours after treatment then declining over the following 3-6 hours. After a 1 hour treatment with 25mM HNE, p53 levels peak at 3 hours while at 75mM HNE p53 levels show no significant increase. RAW 264.7 cells stably expressing the anti-apoptotic protein BCL-2 showed a greater p53 protein accumulation than parental cells after treatment with 50mM HNE. Unlike parental cells, however, p53 levels peaked at 9 hours and remained elevated for 48 hours. The fate of these cells in addition to the effect of elevated p53 on the cell cycle of BCL2 transfectant is discussed.

In addition to p53, cytochrome c release was also examined. After treatment with 50mM HNE, cytosolic levels of cytochrome c increased to approximately 10% of the total amount of releasable cytochrome c. With 75mM HNE a significant amount of release was detected. The BCL2-transfected lines showed no significant increase in cytochrome c release at any HNE concentration.

To further elucidate the role and contribution of the p53 mediated pathway, parental cells were stably transfected with simian virus 40 T antigen (TAG) a known inactivator of p53 function. Although TAG was shown to bind to p53 as well as prevent p53 function (loss of upregulation of downstream mediator p21(*WAF1*)), no discernable differences were seen in apoptosis induction suggesting the importance of a second apoptotic pathway. . *Supported by NIH Grant # CA-76283, and DOD Grant # DAMD 17-98-8286.*

Presented to : American Association for Cancer Research, Conference on Cell Death. Lake Tahoe, NV. Feb. 2000.

Abstract #3 :

Patterns of p53 Accumulation and Cytochrome c Release Upon Induction of Apoptosis by the Lipid Peroxidation Product 4-Hydroxy-2-nonenal in RAW 264.7 cells. Robin L. Haynes and Alan J. Townsend. Biochemistry Dept., Wake Forest Univ. School of Medicine, Winston-Salem, NC 27157.

4-Hydroxy-2-nonenal (HNE), a reactive aldehyde product of the peroxidation of ω–fatty acids, has been shown to induce apoptosis in some cell lines. When RAW 264.7 murine macrophage cells were treated with HNE, apoptosis was induced in a dose-dependent manner, as seen by caspase activation and internucleosomal DNA fragmentation. Since HNE has been suggested to induce DNA damage, p53 levels were examined. After 1 hour at 50μM HNE, p53 levels increased, peaking at 6 hours after treatment, then declining over 3 - 6 hours. At 25 μM HNE, p53 levels peaked at 3 hours while at 75μM, surprisingly, p53 levels were unchanged. RAW 264.7 cells stably expressing the anti-apoptotic protein BCL-2 also showed even higher p53 protein accumulation after 50 μM HNE. However, p53 levels peaked at 9 hours after exposure, and remained elevated for 48 hours. 50uM HNE induced release of approximately 10% of the total amount of available cytochrome c into cytosol. At 75μM HNE a higher amount of release was detected, but without p53 accumulation. The BCL2-transfected lines showed no increase in cytochrome c release at any HNE concentration. These results suggest multiple pathways of HNE-induced apoptosis. *Supported by NIH Grant # CA-76283, and DOD Grant # DAMD 17-98-8286.*

Presented at the April 2000 annual meeting of the American Association for Cancer Research

Abstract #4 :

STRUCTURE-ACTIVITY AND MECHANISTIC STUDIES ON THE TOXICITY OF 4-HYDROXY 2-NONENAL, A BYPRODUCT OF THE PEROXIDATION OF POLYUNSATURATED FATTY ACIDS

Robin L. Haynes and Alan J. Townsend

Wake Forest University Baptist Medical Center
Winston Salem, North Carolina.

The role of cellular oxidant stress in carcinogenesis has recently become the focus of intense study. Oxidative stress is generated through the accumulation of reactive oxidative species (ROS) which interact with cellular molecules and lead to the initiation of downstream reactions and an accumulation of reaction byproducts. Lipid peroxidation, a series of self propagating reactions, is initiated upon the interaction of ROS with the polyunsaturated fatty acids of cellular membranes. This reaction, prominent in tissue with high fat content such as breast tissue, results in a number of byproducts including the most toxic 4 hydroxy-2 nonenal (HNE) which is the focus of the research presented.

HNE is a highly reactive lipid molecule which has been shown to damage both DNA and proteins. HNE contains several structural moieties including an aldehyde, a trans-double bond, a hydroxyl group, and a 9-carbon lipid chain. To better understand the mechanism of HNE toxicity we have examined the contribution of each of these structural components to the overall reactivity using analogous compounds which lack one of more components. Using growth inhibition/ cell survival and apoptosis induction as endpoints we find that the order of toxicity of each component is as follows; C_1-aldehyde>>3,4-double bond>fattty acid chain length> C_4-hydroxyl. The potency of the aldehyde and its importance to the toxicity of the compound is confirmed by studies in which cells overexpressing the lipid aldehyde-metabolizing enzyme aldehyde dehydrogenase-3 show complete protection against HNE induced apoptosis and HNE-protein adduct formation.

In addition to structure-activity correlations we are also studying mechanistic aspects of HNE-induced toxicity. Because HNE is known to damage DNA, we examined the possibility that HNE induced a stabilization/activation of tumor supressor protein, p53. These studies were done in a RAW 264.7 mouse macrophage cell line because of the presence of wildtype p53. We find that p53 levels increase substantially at HNE concentrations between 25 and 50μM but show no increase at the higher concentration of 75 μM. When apoptosis induction is examined as well as p53 stabilization, we find that apoptosis increases with increasing concentrations suggesting the presence of multiple, concentration dependent, pathways of apoptosis induction. Cells stably expressing the anti-apoptotic protein BCL-2 showed a greater increase in p53 protein than parental cells yet showed protection against apoptotic DNA fragmentation. The effect of elevated p53 on the cell cycle of BCL-2 transfectants is currently being studied.

These findings on HNE cellular toxicity contribute to the increasing knowledge of the potential role of oxidative stress in carcinogenesis, and suggest possible opportunities for modulation of cellular defense levels, e.g. modulation of phase 2 detoxifying enzymes, in order to regulate the degree of cell death in either normal or tumor cells.

The U.S. Army Medical Research and Materiel Command supported this work under contract # DAMD-17-98-1-8286.

Presented at the June 2000 Era of Hope meeting, Atlanta, GA.

0026-895X/00/040788-07$3.00/0
MOLECULAR PHARMACOLOGY

Mol Pharmacol 58:788–794, 2000

Vol. 58, No. 4
93/854109
Printed in U.S.A.

Structure-Activity Relationships for Growth Inhibition and Induction of Apoptosis by 4-Hydroxy-2-nonenal in Raw 264.7 Cells

ROBIN L. HAYNES, LUKE SZWEDA, KERRY PICKIN, MARK E. WELKER, and ALAN J. TOWNSEND

Department of Biochemistry, Wake Forest University School of Medicine and Wake Forest University Comprehensive Cancer Center, Winston-Salem, North Carolina (R.L.H., A.J.T.); Department of Physiology and Biophysics, Case Western Reserve University School of Medicine, Cleveland, Ohio (L.S.); and Department of Chemistry, Wake Forest University, Winston-Salem, North Carolina (K.P., M.E.W.)

Received February 22, 2000; accepted June 28, 2000

This paper is available online at http://www.molpharm.org

ABSTRACT

4-Hydroxy-2-nonenal (HNE) is a highly reactive lipid aldehyde byproduct of the peroxidation of cellular membranes. The structure of HNE features three functional groups, a C1 aldehyde, a C2═C3 double bond, and a C4- hydroxyl group, each of which may contribute to the toxicity of the compound. In addition, the length of the aliphatic chain may influence toxic potency by altering lipophilicity. Using analogous compounds that lacked one or more of the structural moieties, the role of each of these structural motifs in the cytotoxicity of HNE was examined in a mouse alveolar macrophage cell line (RAW 264.7) by a cell survival and growth assay. The importance of these functional groups in the potency of HNE for induction of apoptosis was also examined. The rank order of effects on toxicity was C1—aldehyde ≥ C2═C3 double bond ≫ C4—hydroxyl, with parallel results in both the survival/growth inhibition and apoptosis induction assays. The chain length also influenced toxicity in a series of α,β-unsaturated alkenyl aldehydes, with increasing chain length yielding increasing toxicity. To confirm the importance of the aldehyde moiety, and to examine the role of metabolic detoxification in cellular defenses against HNE toxicity, a RAW 264.7 cell line overexpressing human aldehyde dehydrogenase-3 (hALDH3) was generated. This cell line exhibited nearly complete protection against HNE-protein adduct formation as well as HNE-induced apoptosis. These results illustrate the comparative significance of key structural features of HNE in relation to its potent toxicity and induction of apoptosis.

Oxidative stress occurs in biological systems when prooxidant species are not adequately detoxified by antioxidant defenses, resulting in the accumulation of chemically altered macromolecules that may compromise function or cause the demise of the cell. Proteins and particularly the polyunsaturated fatty acids that make up biological membranes are susceptible to oxidative damage. When fatty acids such as arachidonic acid interact with free radicals in the presence of molecular oxygen, a self-propagating lipid peroxidation reaction may be initiated that results in the formation of reactive byproducts such as lipid hydroperoxides and aldehydes. The α,β-unsaturated aldehyde 4-hydroxy-2-nonenal is the most reactive and cytotoxic of the aldehyde byproducts of lipid peroxidation (Benedetti et al., 1980). The C3 position of 4-hydroxy-2-nonenal (HNE) is a highly reactive site for Michael addition reactions with cellular thiols (Witz, 1989), and hence readily forms adducts with glutathione or protein thiols. The terminal aldehyde head group can react with the amino group of lysine or the imidazole nitrogen in histidine, albeit more slowly than the Michael addition at C3. The C4 hydroxyl group can undergo a subsequent cyclization with the C1 aldehyde of the C3-thioether Michael adduct to form a relatively stable thiohemiacetal ring (Esterbauer et al., 1991). HNE has been shown to cause a number of deleterious effects in cells, including glutathione depletion (Cadenas et al., 1983), DNA and RNA synthesis inhibition (Poot et al., 1988), calcium homeostasis disturbances (Benedetti et al., 1984), inhibition of mitochondrial respiration (Humphries et al., 1998), and morphological changes (Gadoni et al., 1993). HNE-induced protein damage has been associated with several pathological conditions, such as ischemia-reperfusion injury (Siems et al., 1995), atherosclerosis (Yla-Herttuala et al., 1989), alcoholic liver disease (Li et al., 1997), Alzheimer's disease (Montine et al., 1997), and cellular aging (Lucas and Szweda, 1998).

This work was supported by United States Public Health Service Grant CA76283 from the National Cancer Institute. Tissue Culture, Analytical Imaging, and Biomolecular Research Core Lab facilities were supported in part by Cancer Center Support Grant 5-P30-CA12197 from the National Cancer Institute.

ABBREVIATIONS: HNE, 4-hydroxy-2-nonenal; DMEM, Dulbecco's minimal essential medium; hALDH3, human aldehyde dehydrogenase 3; PAGE, polyacrylamide gel electrophoresis; ALDH, aldehyde dehydrogenase.

Recently, HNE has been shown to induce apoptosis in certain cell lines (Li et al., 1996; Yildiz et al., 1996; Kruman et al., 1997), suggesting a possible connection between oxidant stress-generated lipid peroxidation byproducts and oxidant stress-induced apoptosis. This observation presents questions regarding the mechanism of HNE initiation of apoptosis and the relative contributions of HNE structural components to the potency of induction of apoptosis. Unique structural features of HNE include the presence of two structural domains, a lipophilic tail, and a polar head comprised of several functional groups. The polar head contains an aldehyde at the C1 position, a double bond between C2 and C3, and a hydroxyl group at the C4 position. These groups may participate independently or cooperatively to interact with cellular molecules. One way to evaluate the importance of each moiety in the toxicity of HNE is to compare the effects of HNE to analogous compounds that either vary in fatty acid chain length or lack a specific functional group. For example, compounds such as *trans*-2-hexenal, *trans*-2-octenal, and *trans*-2-nonenal lack the 4-hydroxyl group, and also vary in fatty acid chain length. Compounds such as nonanal and nonenoic acid lack the C2=C3 double bond or the C1 aldehyde, respectively, in addition to loss of the 4-OH group. The experiments described herein were designed to assess the contribution of HNE structural components to the toxicity of HNE and particularly to their ability to induce apoptosis.

Materials and Methods

Cell Culture and Reagents. Mouse alveolar macrophage RAW 264.7 cells were grown at 37°C in a 5% CO_2 atmosphere in Dulbecco's minimal essential medium (DMEM; GIBCO, Grand Island, NY) supplemented with 10% fetal bovine serum. 4-Hydroxynonenal was kindly provided by the lab of Dr. Herman Esterbauer (University of Graz, Graz, Austria), or purchased from Cayman Chemical (Ann Arbor, MI). Analogous aldehydes *trans*-2-hexenal, *trans*-2-octenal, *trans*-2-nonenal, and nonanal were purchased from Aldrich (Milwaukee, WI); nonenoic acid was purchased from TCI (Portland, OR). Synthesis of 4-hydroxynonanal was via reduction of γ-nonanoic lactone by diisobutylaluminum hydride in toluene (Bloch and Gilbert, 1987). The product was purified by silica chromatography, solvent removed, and the oil characterized by NMR at 25°C in 1:1 CD_3OD: D_2O.

Growth Inhibition/Cell Survival. Cells (1.2×10^6) were treated in suspension in 5 ml of PBS plus chemical agent for 30 min at 37°C. Cells were pelleted by centrifugation (1000 rpm for 5 min) and resuspended in DMEM + 10% fetal bovine serum. Cells (6×10^5) were plated in six-well dishes and allowed to grow for 2 days, at which time cells were released by exposure to trypsin/EDTA and counted.

DNA Fragmentation Assay. Cells were plated at 2×10^6 cells per 60-mm Petri dish. After 16 to 20 h, cells were rinsed and treated with agents in serum-free DMEM. After a 1-h exposure, medium was removed and replaced with DMEM + 10% fetal bovine serum. Cells were allowed to incubate for an additional 9 h, at which time they were harvested in PBS, pH 7.4, and centrifuged at 4°C, 1000 rpm for 5 min. Cells were then lysed in 20 mM EDTA, 100 mM Tris, pH 8.0, and 0.8% sodium lauryl sarcosine and subjected to RNase treatment (0.5 mg/ml for 1 h at 37°C) followed by proteinase K treatment (5 mg/ml for 6–12 h at 55°C). Nonfragmented chromosomal DNA was removed by filtering the lysate through 0.45-μm syringe filters pretreated with 0.2 mg/ml BSA. Fragmented DNA were then precipitated with 0.1 volume of 3 M sodium acetate, pH 5.2, and 2.5 volumes of 100% ethanol. Redissolved DNA was electrophoresed on a 1.8% agarose gel, then stained with ethidium bromide; DNA fluorescence was recorded using a video imaging workstation (Alpha Innotech, San Leandro, CA).

Transfection of Human Aldehyde Dehydrogenase 3. The cDNA for human class 3 aldehyde dehydrogenase (hALDH3) was previously cloned by polymerase chain reaction amplification from human stomach cDNA and subcloned into the *Xho*I site of the ΔpCEP4Δ mammalian expression vector, a derivative of the pCEP4 vector (InVitrogen, Carlsbad, CA) modified to prevent episomal replication and favor host cell integration (Bunting et al., 1994). Both the ΔpCEP4Δ/hALDH3 vector and ΔpCEP4Δ (empty vector) were introduced into RAW 264.7 cells using the cationic liposome reagent Escort (Sigma, St. Louis, MO). Briefly, cells were plated in 100-mm Petri dishes and grown to 70 to 80% confluency. Escort (30–50 μL) was incubated with DNA (15–25 μg) in 800 μL of Opti-MEM transfection medium (GIBCO) for 15 min. Opti-MEM was added to Escort/DNA mixture to a total volume of 8 ml. Cells were then allowed to incubate in transfection medium for 6 h. After 24 h, cells were subcultured and selection medium (DMEM + 10% FBS) was added together with 0.7 mg/ml hygromycin. After 9 to 12 days, hygromycin-resistant colonies were cloned and expanded for aldehyde dehydrogenase (ALDH) screening.

Analysis of ALDH Expression. Enzyme activity assays were performed using crude cytosol as previously described (Bunting et al., 1994) with 1 mM benzaldehyde as a substrate and 1 mM NAD+ as a cofactor. The product of HNE modification by hALDH3 was analyzed by electrospray mass spectrometry after incubation of purified hALDH3 with a similar reaction mixture containing 100 μM HNE as substrate and 200 μM NAD+ as oxidant cofactor. The reaction was followed by the change in absorbance at 340 nm and was essentially complete after 3 min. Whereas the blank (no enzyme) reaction mix had only unreacted HNE (m/z = 154.98), the carboxyl product was almost all 4-hydroxynonenoic acid (m/z = 171.04). For hALDH3 protein detection, 50 μg of total protein was electrophoresed on a 10% SDS-PAGE and transferred to nitrocellulose. The nitrocellulose was probed with a 1:3000 dilution of a rabbit anti-rat class 3 ALDH antisera (kindly provided by Dr. Ronald Lindahl, Univ. of South Dakota, Vermillion, SD) that was cross-reactive with human ALDH-3. After probing with horseradish peroxidase-conjugated goat anti-rabbit secondary antibody (Bio-Rad, Hercules, CA), protein was detected by chemiluminescence (NEN Life Science Products, Boston, MA).

Glutathione Assay. Control or HNE-treated cells were placed on ice, pelleted by low-speed centrifugation, and washed with PBS + 5 mM EDTA. Intracellular GSH content was assayed by the glutathione disulfide reductase method (Tietze, 1969). The assay buffer (0.1 M KPO_4, 1 mM EDTA, pH 7.5) included NADPH (0.4 mM), glutathione disulfide reductase (0.8 units), and 5,5′-dithiobis(2-nitrobenzoate) (0.44 mg/ml). Samples of 1×10^6 cells were lysed in 2% sulfosalicylic acid on ice for 5 min, and centrifuged 12,000*g* for 10 min at 4°. Aliquots of the supernatant were assayed by determining the change in absorbance at 412 nm over a 2-min reaction. A standard curve for each assay was used to calculate nanomoles of GSH per reaction.

HNE Protein Adduct Detection. Cells were plated at 2.5×10^6 cells/60-mm dish; 16 to 20 h later, cells were exposed to agents for 1 h in serum-free medium. FBS was added to 10% at 1 h and cells were allowed to incubate for an additional hour. Cells were harvested in PBS, centrifuged, and the pellets lysed in 50 mM Tris, 5 mM EDTA, and 1 mM phenylmethylsulfonyl fluoride. Lysates were centrifuged at 14,000*g* for 10 min at 4°C, and protein (50 μg/lane) was run on a 10% SDS-PAGE and transferred by semidry electrophoresis to nitrocellulose. Adducts were detected using an anti-HNE/protein adduct antibody (Cohn et al., 1996) at a dilution of 1:2500. After probing with goat anti-rabbit, horseradish peroxidase-conjugated secondary antibody (Bio-Rad) (1:3000) the protein was detected using Renaissance chemiluminescence reagent (NEN Life Science Products).

Results

Cytotoxicity. The contributions of the separate domains or functional groups of HNE to the inhibition of cell survival and growth were assessed using different congeners analogous to HNE but differing in one or more functional groups. Cytotoxicity data for HNE, *trans*-2 nonenal (lacks the OH), nonanal (lacks the C2=C3 double bond), and nonenoic acid (lacks the aldehyde) yielded IC_{50} values of 9.0 ± 1.1 μM, 24 ± 4.3 μM, 308 ± 34.9 μM, and 1770 ± 342 μM, respectively (Fig. 1A). The IC_{50} values for HNE and *trans*-2-nonenal differed by 2.7-fold, reflecting a moderate but significant ($P < .001$) contribution of the hydroxyl group to the toxicity of HNE. Although 4-hydroxynonanal was successfully synthesized via reduction of γ-nonanoic lactone, the compound existed primarily (>98%) in the ring-closed hemiacetal form, and was nontoxic up to 2 mM (data not shown). Hence, in the presence of a 4-hydroxyl group, it was not possible to evaluate the mostly blocked aldehyde in the saturated alkanal, whereas the *trans*-double bond prevents this cyclization in the α,β-unsaturated aldehydes. The difference between the toxicity of *trans*-2-nonenal and its saturated analog nonanal was 13-fold ($P < .0001$), whereas substitution of a carboxyl for the aldehyde group resulted in IC_{50} values that were 5.7-fold higher than with nonanal ($P < .0001$), and 74-fold higher than with *trans*-2-nonenal ($P < .0001$). The effect of the lipophilicity on growth inhibition was examined by exposing cells to analogous α,β-unsaturated aldehydes of different alkenyl chain lengths (Fig. 1B). These experiments showed increased toxicity with increased chain length as shown by IC_{50} values of 99 ± 20 μM, 30 ± 5 μM, and 24 ± 4.4 μM for *trans*-2 hexenal, *trans*-2 octenal, and *trans*-2 nonenal, respectively.

Induction of Apoptosis. Increasing concentrations of HNE were added to culture medium to determine the sensitivity of RAW 264.7 cells to induction of apoptosis, and cellular internucleosomal DNA fragmentation was monitored as an index of apoptosis. This HNE dose-response experiment showed the internucleosomal DNA fragmentation characteristic of apoptosis at HNE concentrations as low as 30 μM (Fig. 2). This response is relatively rapid, occurring as early as 8 h after a 1-h exposure to HNE. As the HNE concentration was increased, the amount of fragmentation increased, indicating a greater fraction of cells undergoing apoptosis. In other cell lines HNE has been shown to rapidly deplete cellular GSH, a condition that could trigger apoptosis as a result of oxidative stress caused by loss of the reducing potential of GSH. In the RAW 264.7 cell line used in these experiments, we have found that exposure to 25, 50, and 75 μM HNE resulted in only moderate depletion of total cellular GSH (84.0 ± 6.8, 71.7 ± 5.2, and 68.8 ± 4.5% of GSH levels in control cells, respectively).

Activation of the proapoptotic protease caspase 3 was also examined as a biochemical index of apoptotic response to HNE exposure. Caspase activities of 0.31 nmol/min/mg, 0.64 nmol/min/mg, and 0.79 nmol/min/mg were measured after exposure to 0 μM, 40 μM, and 70 μM HNE, respectively (data not shown). This experiment confirms the dose-dependent nature of the response and also documents a second positive apoptotic endpoint in support of the conclusion that cells are dying by apoptotic rather than necrotic death. In addition, we have used time-lapse video microscopy to show that at 50 μM HNE, more than 90% of the cells have formed apoptotic blebs, blistered, and lysed within 18 h after exposure to HNE (R. L. Haynes and M. Willingham, unpublished observations). These observations confirm that apoptosis is the primary mode of cell death in RAW 264.7 cells after exposure to HNE.

Structure-Activity Correlation with Induction of Apoptosis. The growth inhibition studies provided an index of the relative overall toxicity of each of the compounds and the effect of modification of specific functional groups. A parallel series of experiments was performed to determine whether this relationship is explained by similar effects of these structurally distinct analogs on the degree of induction of apopto-

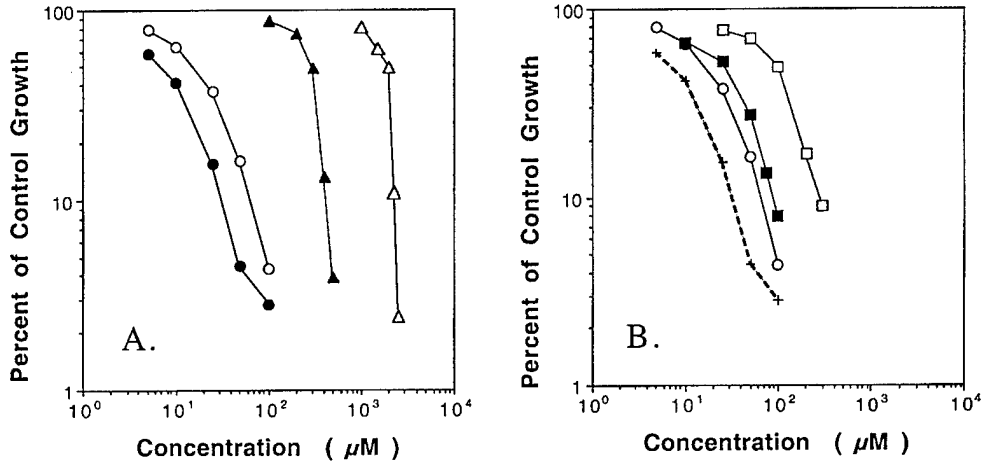

Fig. 1. A, growth inhibition/cell survival to determine the importance of individual functional groups. Cells were dosed with analogous compounds for 30 min as described under *Materials and Methods* and allowed to grow for 2 days, at which time they were trypsinized and counted. Analogous compounds used include HNE (●); *trans*-2-nonenal (○) (lacks the hydroxyl); nonanal (▲) (lacks the C2=C3 double bond and hydroxyl); and nonenoic acid (△) (lacks the C1 aldehyde and hydroxyl. Respective IC_{50} values are 9.0 ± 1.1 μM, 24 ± 4.3 μM, 308 ± 34.9 μM, and 1770 ± 342 μM. The results are mean ± S.E. for four to seven separate experiments. B, growth inhibition/cell survival to determine the importance of chain length. Cells were dosed for 30 min as described under *Materials and Methods* with analogous aldehydes *trans*-2-nonenal (○) (nine carbons), *trans*-2-octenal (■) (eight carbons), and *trans*-2-hexenal (□) (six carbons). The dashed line is the HNE data from A, for comparison. IC_{50} values are 24 ± 4.3, 30 ± 5, and 99 ± 20 μM for *trans*-2-nonenal, *trans*-2-octenal, and *trans*-2-hexenal, respectively. The results are mean ± S.E. for five separate experiments.

sis compared with HNE. To determine the extent to which the various functional groups influence this apoptotic induction, a dose-response experiment was carried out using the same compounds as in Fig. 1A, but with DNA fragmentation as an index of apoptosis. As the HNE exposure was increased, there was a progressive increase in apoptosis induction over the range of 25 to 75 μM (Fig. 3). *trans*-2-Nonenal yields a dose-response relationship similar to that of HNE, confirming the similar toxicity of these two 9-carbon, α,β-unsaturated aldehydes, with only modest loss of apoptotic efficacy in the absence of the hydroxyl group. Neither nonanal nor nonenoic acid induced any apoptotic DNA fragmentation within the concentration range tested (25–75 μM). However, as shown in Fig. 1A, these concentrations may not be toxic enough to induce significant amounts of apoptosis. Indeed, cells treated with nonanal or nonenoic acid concentrations in the IC_{50} to IC_{90} range exhibited significant DNA fragmentation (data not shown), indicating an apoptotic mode of cell death with these compounds as well. The role of hydrophobicity in HNE-induced apoptosis was also examined for α,β-unsaturated aldehydes of different chain lengths, with DNA fragmentation as an endpoint. *trans*-2-Hexenal yielded very little apoptosis induction in the concentration range tested. Increasing the length of the chain by two carbons (*trans*-2-octenal) resulted in a significant increase in DNA fragmentation, and addition of a ninth carbon (*trans*-2-nonenal) further enhanced the apoptotic induction (Fig. 4). These results parallel the growth inhibition data seen in Fig. 2B, with increased apoptotic induction in parallel with increasing chain length in the order *trans*-2-hexenal < *trans*-2-octenal < *trans*-2-nonenal.

The nonenoic acid used to examine the effect of loss of the aldehyde group also lacked a 4-hydroxyl group; hence, it is not strictly analogous to HNE as a monofunctionally modified congener. Consequently, the role of the aldehyde in the toxicity of HNE was also examined by an indirect approach. We have previously found that expression of an hALDH3 conferred strong protection against HNE toxicity when expressed via stable transfection in V79 hamster lung fibroblast cells (K. D. Bunting, R. L. Haynes, L. Szweda, W. G. Jerome, and A. J. Townsend, unpublished results). We also showed that crude cytosol from these cells supported oxidation of NAD+ with HNE as substrate and that purified hALDH3 catalyzed a facile and essentially complete NAD-dependent oxidation of HNE to 4-hydroxynonenoic acid, as verifed by mass spectrometry (K. D. Bunting, R. L. Haynes, L. Szweda, W. G. Jerome, and A. J. Townsend, unpublished results). The same expression vector was used to express hALDH3 by stable transfection in RAW 264.7 cells, as shown in Fig. 5, by comparison of the clone hALDH3-109 to the empty vector-transfected control ΔpCEP4Δ-16. Activity assays yielded an ALDH activity of 100 ± 4 mU/mg in clone 109 compared with undetectable activity in the control line. When control and hALDH3-transfected cells were exposed to HNE, expression of hALDH3 protected against apoptosis induction throughout the concentration range tested (Fig. 6A). The protection provided by hALDH3 expression was

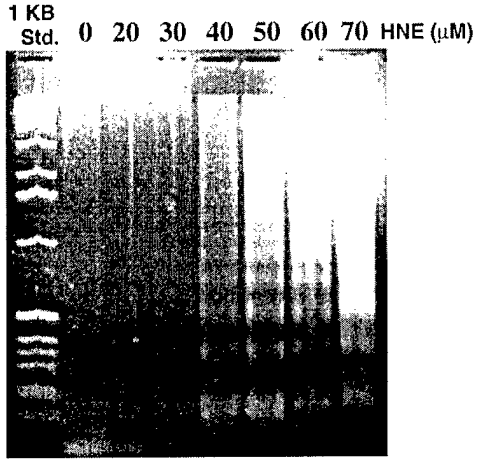

Fig. 2. Internucleosomal DNA fragmentation induced by HNE. RAW 264.7 cells were treated with increasing concentrations of HNE for 1 h in serum-free medium and then medium was replaced with fresh complete medium without HNE. Nine hours after removal of HNE, cells were harvested and DNA was isolated, electrophoresed, and stained with ethidium bromide as described under *Materials and Methods*.

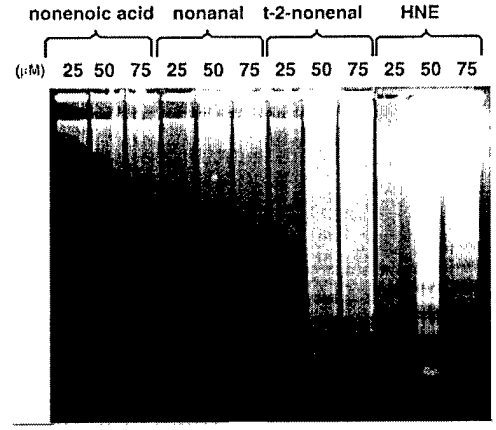

Fig. 3. Internucleosomal DNA fragmentation induced by 9-carbon analogs of HNE. Cells were exposed for 1 h in serum-free medium containing the indicated concentrations of one of the following compounds: nonenoic acid (lacks the C1 aldehyde and hydroxyl), nonanal (lacks the C2=C3 double bond and hydroxyl), *trans*-2 nonenal (lacks the hydroxyl), or HNE. Cells were harvested and DNA was isolated, electrophoresed, and stained with ethidium bromide as described under *Materials and Methods*.

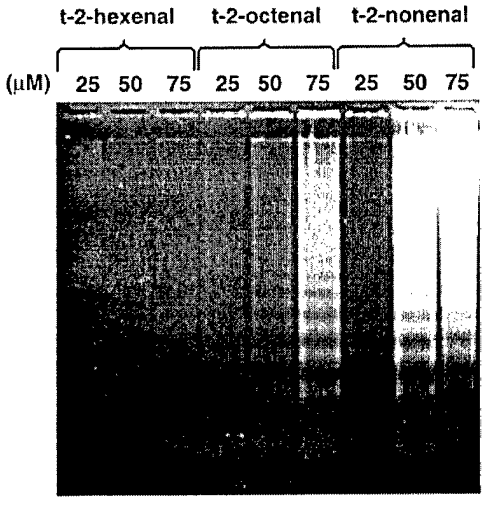

Fig. 4. Internucleosomal DNA fragmentation induced by lipid aldehydes of increasing chain length. Cells were exposed for 1 h in serum-free medium containing the indicated concentrations of one of the following lipid aldehydes: *trans*-2-hexenal (six carbons), *trans*-2-octenal (eight carbons), or *trans*-2-nonenal (nine carbons). Cells were harvested 9 h after removal of HNE and DNA was isolated, electrophoresed, and stained with ethidium bromide as described under *Materials and Methods*.

further characterized by measurement of HNE-protein adducts formed in each cell line. The HNE-protein adducts were detected by Western blotting with an antibody specific for the products of reactions between HNE and protein thiols, amino groups, and histidine residues (Uchida et al., 1993). Figure 6B shows the dose-dependent nature of HNE-protein adduct formation in the empty vector-transfected ΔpCEP4Δ-16 control line. Cells overexpressing hALDH3 were essentially completely protected, as evidenced by extremely low levels of adduct formation throughout the concentration range tested. This protection is consistent with the demonstrated conversion of HNE to the carboxylic acid congener by hALDH3, in light of the earlier toxicity and apoptosis experiments that indicated far less toxicity with nonenal than nonenoic acid in the series of 9-carbon compounds tested.

Discussion

The chemical reactions with macromolecules such as protein and DNA that underlie the biological effects of many of the major lipid peroxidation products have been well characterized (Witz, 1989; Esterbauer et al., 1991; Esterbauer, 1993). The α,β-unsaturated aldehydes such as HNE react with a range of macromolecules but to widely varying extents depending on the reaction chemistry of the interacting functional groups and microenvironmental factors (e.g., accessibility, hydration, pH, proximity of other functional groups) (Witz, 1989; Esterbauer et al., 1991). The β-carbon (C3) and the carbonyl center (C1) readily undergo nucleophilic addition of thiols, and amino groups can also form adducts at the C1 or C3 carbon atoms via Schiff base or Michael addition reactions, respectively (Esterbauer et al., 1991; Witz, 1989). The interaction of HNE with proteins is complex because of the multiple reactive groups comprising the polar head of HNE, which allows for crosslinks between functional groups such as thiols, amino groups, and histidine residues. Structure-activity comparisons with compounds related to HNE have been used previously to assess the contribution of individual functional groups to the biological effects of HNE, with somewhat variable results, depending on the toxic endpoint examined (Hauptlorenz et al., 1985; Brambilla et al., 1986; Kaneko et al., 1988). Our present studies have focused on the structural contributions to induction of apoptosis compared with the effects of these structural determinants on survival and subsequent growth in a murine macrophage cell line.

The cytotoxicity assay demonstrated that substitution of a carboxyl group for the aldehyde caused the greatest decrease in toxicity among the structural analogs studied. This is shown by the dramatic decrease in toxicity when cells are exposed to nonenoic acid, which lacks the aldehyde yet retains the double bond (IC_{50} of 1770 μM) compared with *trans*-2-nonenal (IC_{50} of 24 μM). Consistent with this observation, no apoptosis (as evidenced by DNA fragmentation) was induced by nonenoic acid up to 75 μM, which resulted in more than 90% apoptotic cells with HNE or *trans*-2-nonenal. Although a significant fraction of cells became apoptotic at millimolar concentrations near the IC_{50} value (data not shown), this could have been caused by nonspecific detergent-like effects of nonenoic acid on the integrity of the plasma membrane. Alternatively, the RAW 264.7 cell line

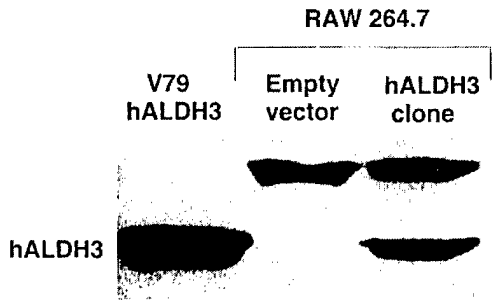

Fig. 5. Expression of hALDH3. Cytosolic protein (50 μg/lane) from control RAW 264.7 cells transfected with a ΔpCEP4Δ control (empty) vector (lane 2) or cells transfected with a ΔpCEP4Δ vector containing human ALDH3 cDNA (lane 3) was run on a 10% SDS-PAGE and transferred to nitrocellulose and probed with 1:3000 dilution of tALDH antisera. Enzyme activity was undetectable in control cells and 100 ± 4 mU/mg in the ALDH3 expressing clonal line. A V79 cell line overexpressing hALDH3 (Bunting and Townsend, 1996) was used as a positive control (lane 1). The upper band is a nonspecific cross-reacting protein present in RAW 264.7 cells.

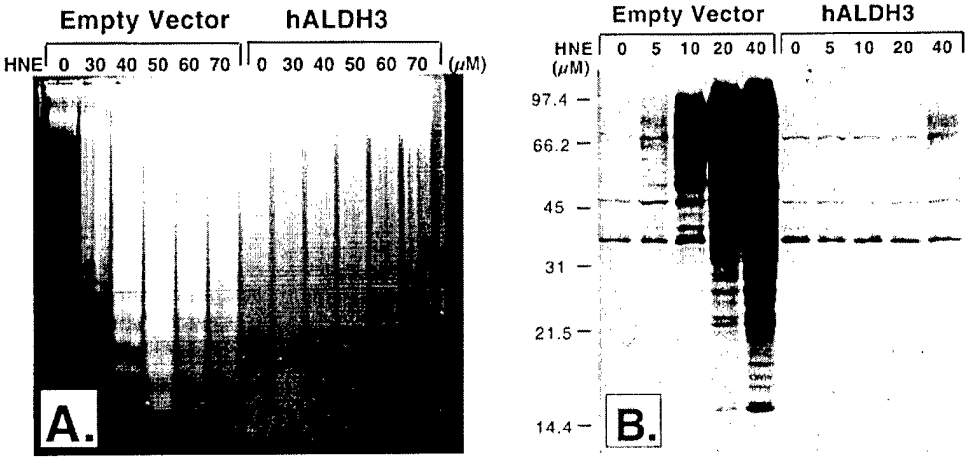

Fig. 6. A, ALDH protection against HNE-induced DNA fragmentation. Control empty vector-transfected RAW 264.7 cells or cells overexpressing hALDH3 were exposed to increasing concentrations of HNE for 1 h in serum-free medium. Cells were harvested 9 h after removal of HNE, and DNA was isolated, electrophoresed, and stained with ethidium bromide as described under *Materials and Methods*. B, ALDH protection against HNE-induced protein adduct formation. Control empty vector-transfected RAW 264.7 cells or cells overexpressing hALDH3 were exposed to increasing concentrations of HNE for 1 h in serum-free medium. Cells were lysed and cytosolic protein (50 μg/lane) was electrophoresed on a 10% SDS-PAGE and transferred to nitrocellulose. Protein adducts were probed using an antibody specific for HNE adducts, diluted 1:2500, as described under *Materials and Methods*.

may have a propensity toward the apoptotic mode of cell death. However, induction of apoptosis by HNE also occurs in several other cell types, including alveolar macrophages (Li et al., 1996), neuronal cells (Kruman et al., 1997), and endothelial cells (Herbst et al., 1999), suggesting that a specific mechanism of apoptosis induction may be activated.

Two potentially interrelated factors could explain the major loss of potency in the absence of the aldehyde. First, a common effect of exposure of cells to HNE is facile alkylation of protein thiols and also nonprotein thiols such as glutathione (Cadenas et al., 1983; Witz, 1989; Esterbauer et al., 1991). In the Michael addition reaction, the electron-withdrawing effect of the adjacent aldehyde facilitates the addition of a nucleophilic thiol or amino group across the C2=C3 double bond. Substitution of the more electron-rich carboxyl for the C1-aldehyde greatly reduces the reactivity of the double bond, resulting in decreased Michael addition reaction. Second, the reduced toxicity may in part reflect loss of the ability to form crosslinks, because the aldehyde is no longer available as a second site of adduction, leaving only the greatly weakened addition site at the double bond remaining. In the case of HNE, loss of the C1 aldehyde also prevents the intramolecular cyclization that can occur between the C1 carbon and the C4 hydroxyl after Michael addition of a thiol. This structure probably stabilizes the thioether linkage of the adduct.

The importance of the C2=C3 double bond was illustrated by exposure to nonanal, a 9-carbon alkyl analog that retains the aldehyde but lacks the double bond and C4 hydroxyl. The toxicity (IC_{50} of 308 μM) with the aldehyde alone was intermediate between *trans*-2-nonenal (IC_{50} of 24 μM) and nonenoic acid (IC_{50} of 1770 μM). Thus, although the loss of the aldehyde in nonenoic acid resulted in a 74-fold decrease in toxicity compared with *trans*-2-nonenal, the lack of a double bond in nonanal decreased toxicity by 13-fold relative to *trans*-2-nonenal. Again, similar results were observed for induction of apoptosis, with no internucleosomal DNA fragmentation at concentrations up to 75 μM nonanal or nonenoic acid but significant apoptosis in the IC_{50} range (data not shown). The loss of the double bond prevents Michael additions at the C3 position and also removes its potentiation of the reactivity of the aldehyde. Saturated aldehydes can interact with proteins to form Schiff base adducts, but these reactions occur more slowly and are more readily reversible than the Michael additions, hence the intermediate toxicity of nonanal. The results with nonenoic acid, *trans*-2-nonenal, and nonanal indicated that both the aldehyde and the C2=C3 double bond are essential for the full toxicity of HNE and induction of apoptosis and also that their effects are additive and mutually interactive.

A third reactive group, the 4-hydroxyl, apparently contributes somewhat less to the toxicity of HNE, as evidenced by the 2.7-fold decrease in the toxicity of *trans*-2-nonenal compared with HNE (IC_{50} of 24 μM versus 9 μM for HNE) and the parallel difference for induction of apoptotic DNA fragmentation for these two analogs. Previously published results showed only a slight difference for inhibition of human umbilical vein endothelial cell growth by *trans*-2-nonenal and HNE (Kaneko et al., 1988), and about 2-fold greater toxicity of HNE when survival of human diploid fibroblasts was the measured toxicity endpoint (Kaneko et al., 1987). In the mechanism of the HNE reaction with thiols, the 4-hydroxyl group contributes to the reactivity of the Michael addition site by acting as an electron-withdrawing group to increase the reactivity of the double bond for Michael additions at C3. Secondly, it may stabilize the resulting adduct by participating in an intramolecular cyclization with the aldehyde to yield a cyclic hemiacetal product that is in tautomeric equilibrium with the open chain aldehyde. With *trans*-2-nonenal, the final product is a linear adduct at the C3 position; this may be less stable and more readily reversible (and therefore less toxic) than HNE. The effect of the 4-hydroxyl on the toxicity of the saturated 4-hydroxynonanal could not be evaluated because of cyclization of the chemically synthesized compound, but it would be expected to have minimal effect anyway, because there is no adjacent double bond to be influenced by its electron-withdrawing effect, and the aldehyde is separated by two saturated carbon atoms.

The importance of the length of the alkenyl chain was apparent from the decreasing IC_{50} values in the toxicity assay as the length increased from six to nine carbons, and the parallel effects on induction of apoptosis. Hydrophobicity constants for each of the lipid aldehydes used in this study are 0.85 for *trans*-2-hexenal, 1.89 for *trans*-2 octenal, 2.30 for *trans*-2-nonenal, and 1.01 for HNE (Bounds and Winston, 1991). Thus, although the alkenals are progressively correlated with hydrophobicity, the lack of correlation with HNE indicates that this factor contributes to rather than causes toxicity.

The observation that more than 90% of cells treated with 75 μM HNE ultimately undergo apoptosis is consistent with the parallel results of the cytotoxicity and apoptosis studies, with entirely analogous structure-activity relationships for the potency of the apoptotic induction. The concentration of HNE required to induce apoptosis was severalfold higher than the IC_{50} for the survival and growth assay, most likely because of a difference in the exposure conditions. The cells were at a higher density for the apoptosis experiments, a variable that is known to affect the absolute toxicity of α,β-unsaturated aldehydes (Esterbauer et al., 1991; Norton et al., 1997). Another factor is that the cells were already attached in a monolayer for the apoptosis assay, with less surface area available and the potentially protective advantage of cell-cell interactions, whereas the exposure for the cytotoxicity assay was in suspension. Measured overall concentrations of HNE in cell cytosol of nonstressed cells or tissues are typically in the low micromolar range (Esterbauer et al., 1991). However, significantly higher concentrations were found in human monocytes, which generate large amounts of reactive oxygen species, and it is has been estimated that localized HNE concentrations can increase to as high as 4.5 mM within peroxidizing membrane bilayers (Esterbauer et al., 1991). Thus, mitochondrial membranes may accumulate high HNE concentrations because of the nearness of reactive oxygen species released during normal oxidative energy metabolism. During oxidant stress, key mitochondrial proteins such as cytochrome *c* oxidase and the adenine nucleotide transporter have been shown to be alkylated by HNE to a greater extent (Chen et al., 1995, 1998). Changes in mitochondrial function have also been associated with exposure to lipid peroxidation products, including HNE, in mitochondria (Richter and Meier, 1990; Ullrich et al., 1996; Keller et al., 1997; Humphries et al., 1998), and HNE has been shown to induce the mitochondrial permeability transition that is believed to

be an irreversible event in the induction of apoptosis (Kristal et al., 1996; Marchetti et al., 1996a,b).

Exposures to the toxic compounds used in this study were via addition to the extracellular medium; thus, it was of interest to verify that the aldehyde group exerted its toxicity intracellularly, rather than at the plasma membrane. Stable expression of hALDH3, an HNE oxidizing enzyme, via transfection into RAW 264.7 cells completely protected the cells from apoptotic induction to at least 70 μM HNE, compared with the nonexpressing control cells. This confirms the idea that the principal targets for the toxic effects are intracellular, because ALDH-3 is cytosolic and would not be expected to protect surface membrane components or functions from extracellular HNE. Analysis of HNE-protein adduct formation showed potent protection against protein damage by hALDH3 expression, presumably because of oxidation of the aldehyde to the far less reactive carboxylic acid. This observation suggests that protein modification likely plays a direct causative role as a trigger mechanism for the apoptotic induction. Modification of key thiol groups in mitochondrial proteins, such as the permeability transition pore, has been proposed as a trigger mechanism that initiates the role of this organelle in apoptosis (Petronilli et al., 1994; Costantini et al., 1996; Zamzami et al., 1998). Studies are currently in progress to investigate the role of acute damage to mitochondria in the mechanism of HNE induction of apoptosis.

References

Benedetti A, Comporti M and Esterbauer H (1980) Identification of 4-hydroxynonenal as a cytotoxic product originating from the peroxidation of liver microsomal lipids. *Biochim Biophys Acta* **620**:281–296.

Benedetti A, Fulceri R and Comporti M (1984) Inhibition of calcium sequestration activity of liver microsomes by 4-hydroxyalkenals originating from the peroxidation of liver microsomal lipids. *Biochim Biophys Acta* **793**:489–493.

Bloch R and Gilbert L (1987) Synthesis of both enantiomers of γ-substituted α, β-unsaturated γ-lactones. *J Org Chem* **52**:4603–4605.

Bounds PL and Winston GW (1991) The reaction of xanthine oxidase with aldehydic products of lipid peroxidation. *Free Radic Biol Med* **11**:447–453.

Brambilla G, Sciaba L, Faggin P, Maura A, Marinari UM, Ferro M and Esterbauer H (1986) Cytotoxicity, DNA fragmentation and sister-chromatid exchange in Chinese Hamster Ovary cells exposed to the lipid peroxidation product 4-hydroxynonenal and homologous aldehydes. *Mutat Res* **171**:169–176.

Bunting KD, Lindahl R and Townsend AJ (1994) Oxazaphosphorine-specific resistance in human MCF-7 breast carcinoma cell lines expressing transfected rat class 3 aldehyde dehydrogenase. *J Biol Chem* **269**:23197–23203.

Bunting KD and Townsend AJ (1996) Protection by transfected rat or human class 3 aldehyde dehydrogenases against the cytotoxic effects of oxazaphosphorine alkylating agents in hamster V79 cell lines—Demonstration of aldophosphamide metabolism by the human cytosolic class 3 isozyme. *J Biol Chem* **271**:11891–11896.

Cadenas E, Muller A, Brigelius R, Esterbauer H and Sies H (1983) Effects of 4-hydroxynonenal on isolated hepatocytes. *Biochem J* **214**:479–487.

Chen JJ, Bertrand H and Yu BP (1995) Inhibition of adenine nucleotide translocator by lipid peroxidation products. *Free Radic Biol Med* **19**:583–590.

Chen J, Schenker S, Frosto TA and Henderson GI (1998) Inhibition of cytochrome c oxidase activity by 4-hydroxynonenal (HNE). Role of HNE adduct formation with the enzyme subunits. *Biochim Biophys Acta* **1380**:336–344.

Cohn JA, Tsai L, Friguet B and Szweda LI (1996) Chemical characterization of a protein-4-hydroxy-2-nonenal cross-link: Immunochemical detection in mitochondria exposed to oxidative stress. *Arch Biochem Biophys* **328**:158–164.

Costantini P, Chernyak B, Petronilli V and Bernardi P (1996) Modulation of the mitochondrial permeability transition pore by pyridine nucleotides and dithiol oxidation at 2 separate sites. *J Biol Chem* **271**:6747–6751.

Esterbauer H (1993) Cytotoxicity and genotoxicity of lipid-oxidation products. *Am J Clin Nutr* **57 (5 Suppl)**:779S–786S.

Esterbauer H, Schaur RJ and Zollner H (1991) Chemistry and biochemistry of 4-hydroxynonenal, malonaldehyde and related aldehydes. *Free Radic Biol Med* **11**:81–128.

Gadoni E, Olivero A, Miglietta A, Bocca C and Gabriel L (1993) Cytoskeletal modifications induced by 4-hydroxynonenal. *Cytotechnology* **11**:S62–S64.

Hauptlorenz S, Esterbauer H, Moll W, Pumpel R, Schauenstein E and Puschendorf B (1985) Effects of the lipid peroxidation product 4-hydroxynonenal and related aldehydes on proliferation and viability of cultured Ehrlich ascites tumor cells. *Biochem Pharmacol* **34**:3803–3809.

Herbst U, Toborek M, Kaiser S, Mattson MP and Hennig B (1999) 4-hydroxynonenal induces dysfunction and apoptosis of cultured endothelial cells. *J Cell Physiol* **181**:295–303.

Humphries KM, Yoo Y and Szweda LI (1998) Inhibition of NADH-linked mitochondrial respiration by 4-hydroxy-2-nonenal. *Biochemistry* **37**:552–557.

Kaneko T, Honda S, Nakano S-I and Matsuo M (1987) Lethal effects of linoleic acid hydroperoxide and its autoxidation products, unsaturated aliphatic aldehydes, on human diploid fibroblasts. *Chem-Biol Interact* **63**:127–137.

Kaneko T, Kaji K and Matsuo M (1988) Cytotoxicities of a linoleic acid hydroperoxide and its related aliphatic aldehydes toward cultured human umbilical vein endothelial cells. *Chem-Biol Interact* **67**:295–304.

Keller JN, Pang Z, Geddes JW, Begley JG, Germeyer A, Waeg G and Mattson MP (1997) Impairment of glucose and glutamate transport and induction of mitochondrial oxidative stress and dysfunction in synaptosomes by amyloid beta-peptide: Role of the lipid peroxidation product 4-hydroxynonenal. *J Neurochem* **69**:273–284.

Kristal BS, Park BK and Yu BP (1996) 4-Hydroxyhexenal is a potent inducer of the mitochondrial permeability transition. *J Biol Chem* **271**:6033–6038.

Kruman I, Bruce-Keller AJ, Bredesen D, Waeg G and Mattson MP (1997) Evidence that 4-hydroxynonenal mediates oxidative stress-induced neuronal apoptosis. *J Neurosci* **17**:5089–5100.

Li L, Hamilton RF Jr, Kirichenko A and Holian A (1996) 4-Hydroxynonenal-induced cell death in murine alveolar macrophages. *Toxicol Appl Pharmacol* **139**:135–143.

Li CJ, Nanji AA, Siakotos AN and Lin RC (1997) Acetaldehyde-modified and 4-hydroxynonenal-modified proteins in the livers of rats with alcoholic liver disease. *Hepatology* **26**:650–657.

Lucas DT and Szweda LI (1998) Cardiac reperfusion injury: Aging, lipid peroxidation, and mitochondrial dysfunction. *Proc Natl Acad Sci USA* **95**:510–514.

Marchetti P, Castedo M, Susin S, Zamzami N, Hirsch T, Macho A, Haeffner A, Hirsch F, Geusekns M and Kroemer G (1996a) Mitochondrial permeability transition is a central coordinating event of apoptosis. *J Exp Med* **184**:1155–1160.

Marchetti P, Hirsch T, Zamzami N, Castedo M, Decaudin D, Susin S, Masse B and Kroemer G (1996b) Mitochondrial permeability transition triggers lymphocyte apoptosis. *J Immunol* **157**:4830–4836.

Montine KS, Olson SJ, Amarnath V, Whetsell WO Jr, Graham DG and Montine TJ (1997) Immunohistochemical detection of 4-hydroxy-2-nonenal adducts in Alzheimer's disease is associated with inheritance of APOE4. *Am J Pathol* **150**:437–443.

Norton ND, Mamiya BM and Kehrer JP (1997) Relationships between cell density, glutathione and proliferation of A549 human lung adenocarcinoma cells treated with acrolein. *Toxicology* **122**:111–122.

Petronilli V, Costantini P, Scorrano L, Colonna R, Passamonti S and Bernardi P (1994) The voltage sensor of the mitochondrial permeability transition pore is tuned by the oxidation-reduction state of vicinal thiols. Increase of the gating potential by oxidants and its reversal by reducing agents. *J Biol Chem* **269**:16638–16642.

Poot M, Verkerk A, Koster J, Esterbauer H and Jongkind J (1988) Reversible inhibition of DNA and protein synthesis by cumene hydroperoxide and 4-hydroxynonenal. *Mech Ageing Dev* **43**:1–9.

Richter C and Meier P (1990) Inhibition of pro-oxidant-induced mitochondrial pyridine nucleotide hydrolysis and calcium release by 4-hydroxynonenal. *Biochem J* **269**:735–737.

Siems WG, Grune T and Esterbauer H (1995) 4-Hydroxynonenal formation during ischemia and reperfusion of rat small intestine. *Life Sci* **57**:785–789.

Tietze F (1969) Enzymic method for quantitative determination of nanogram amounts of total and oxidized glutathione. *Anal Biochem* **27**:502–522.

Uchida K, Szweda LI, Chae HZ and Stadtman ER (1993) Immunochemical detection of 4-hydroxynonenal protein adducts in oxidized hepatocytes. *Proc Natl Acad Sci USA* **90**:8742–8746.

Ullrich O, Henke W, Grune T and Siems WG (1996) The effect of the lipid peroxidation product 4-hydroxynonenal and of its metabolite 4-hydroxynonenoic acid on respiration of rat kidney cortex mitochondria. *Free Radic Res* **24**:421–427.

Witz G (1989) Biological interactions of alpha, beta-unsaturated aldehydes. *Free Radic Biol Med* **7**:333–349.

Yildiz D, Ercal N, Frank RL and Matthews RH (1996) Effects of 4-hydroxynonenal and *N*-acetyl-L-cysteine on Myc-induced apoptosis. *Toxicol Lett* **89**:215–221.

Yla-Herttuala S, Palinski W, Rosenfeld ME, Parthasarathy S, Carew TE, Butler S, Witztum JL and Steinberg D (1989) Evidence for the presence of oxidatively modified low density lipoprotein in atherosclerotic lesions of rabbit and man. *J Clin Invest* **84**:1086–1095.

Zamzami N, Marzo I, Susin SA, Brenner C, Larochette N, Marchetti P, Reed J, Kofler R and Kroemer G (1998) The thiol crosslinking agent diamide overcomes the apoptosis-inhibitory effect of Bcl-2 by enforcing mitochondrial permeability transition. *Oncogene* **16**:1055–1063.

Send reprint requests to: Alan J. Townsend, Ph.D., Biochemistry Department, Wake Forest University School of Medicine, Medical Center Blvd., Winston-Salem, NC 27157. E-mail: atown@wfubmc.edu

ELSEVIER

Chemico-Biological Interactions 000 (2000) 000–000

Chemico-Biological Interactions

www.elsevier.com/locate/chembiont

Selective protection by stably transfected human ALDH3A1 (but not human ALDH1A1) against toxicity of aliphatic aldehydes in V79 cells

Alan J. Townsend [a,*], Sandra Leone-Kabler [a], Robin L. Haynes [a], Yinghui Wu [a], Luke Szweda [b], Kevin D. Bunting [a]

[a] *Biochemistry Department, Wake Forest University School of Medicine, Medical Center Blvd., Winston-Salem, NC 27157, USA*

[b] *Department of Physiology and Biophysics, Case Western Reserve School of Medicine, 10900 Euclid Ave., Cleveland, OH, 44106-4970, USA*

Abstract

Toxic medium chain length alkanals, alkenals, and 4-hydroxyalkenals that are generated during lipid peroxidation are potential substrates for aldehyde dehydrogenase (ALDH) isoforms. We have developed transgenic cell lines to examine the potential for either human ALDH1A1 or ALDH3A1 to protect against damage mediated by these toxic aldehydes. Using crude cytosols from stably transfected cell lines, these aldehydes were confirmed to be excellent substrates for ALDH3A1, but were poorly oxidized by ALDH1A1. Expression of ALDH3A1 by stable transfection in V79 cells conferred a high level of protection against growth inhibition by the medium-chain length aldehyde substrates with highest substrate activity, including hexanal, trans-2-hexenal, trans-2-octenal, trans-2-nonenal, and 4-hydroxy-2-nonenal (HNE). This was reflected in a parallel ability of ALDH3A1 to prevent depletion of glutathione by these aldehydes. Expression of hALDH3 completely blocked the potent

Abbreviations: ALDH, aldehyde dehydrogenase; DMEM, dulbecco's modified minimum essential medium; DTNB, 5'5'-dithio-bis-(2-nitrobenzoic acid); GSH, reduced glutathione; GST, glutathione S-transferase; HA, hexanal; HNE, 4-hydroxy-2-nonenal; LPO, lipid peroxidation; MDA, malondialdehyde; PBS, phosphate-buffered saline; t2HE, *trans*–2-hexenal; t2OE, *trans*–2-octenal; t2NE, *trans*–2-nonenal; TCA, trichloroacetic acid.

* Corresponding author: Fax: + 1-336-7167671.

E-mail address: atown@wfubmc.edu (A.J. Townsend).

PII: S0009-2797(00)00270-2

induction of apoptosis by HNE in both V79 cells and in a RAW 264.7 murine macrophage cell line, consistent with the observed total prevention of HNE-protein adduct formation. Structure–activity studies indicated that the rank order of potency for the contributions of HNE functional groups to toxicity was aldehyde $\geq$ C2 = C3 double bond > > C4-hydroxyl group. Oxidation of the aldehyde moiety of HNE to a carboxyl by ALDH3A1 expressed in stably transfected cell lines drastically reduced its potency for growth inhibition and apoptosis induction. In contrast, ALDH1A1 expression provided only moderate protection against trans-2-nonenal (t2NE), and none against the other six–nine carbon aldehydes. Neither ALDH1A1 nor ALDH3A1 conferred any protection against acrolein, acetaldehyde, or chloroacetaldehyde. A small degree of protection against malondialdehyde was afforded by ALDH1A1, but not ALDH3A1. Paradoxically, cells expressing ALDH3A1 were 1.5-fold more sensitive to benzaldehyde toxicity than control V79 cells. These studies demonstrate that expression of class 3 ALDH, but not class 1 ALDH, can be an important determinant of cellular resistance to toxicity mediated by aldehydes of intermediate chain length that are produced during lipid peroxidation.

Keywords: Human ALDH3; Hydroxyalkenals; Lipid aldehydes; Detoxification; Chemoprevention

1. Introduction

Free radical attack on polyunsaturated fatty acids can initiate lipid peroxidation (LPO) chain reactions that result in the generation of highly reactive radical intermediates, which in turn can give rise to potentially toxic cleavage products including alkanes, alkenes, aldehydes, ketones, and hydroxy-acids [1–4]. Aldehydes comprise a major portion of the carbonyl products. The most common aldehyde formed is malondialdehyde (MDA) which typically comprises 70% of the total aldehydes produced [1]. The major saturated alkyl aldehyde formed is hexanal (HA) [5] (15% of total aldehydes), and the most cytotoxic aldehyde generated is 4-hydroxy-2-nonenal (HNE; 5% of total aldehydes) [1,5,6]. The reactivity of lipid aldehydes increases in the following order: alkanals < alkenals < 4-hydroxyalkenals [1,5]. Alkanals are least reactive and have weaker effects on growth inhibition than unsaturated aldehydes. Alkenals are typically an order of magnitude more reactive than the alkanals, but are produced at lower levels; hence it has been suggested that the overall toxic effects of the alkanals and alkenals may be similar [7]. 4-hydroxy-2-alkenals are the most reactive lipid aldehydes characterized and are highly cytotoxic at low μM concentrations, due to the synergistic interaction between the electrophilic double bond, the hydroxyl group, and the aldehyde moiety [8,9]. In particular, the reactivity of the α,β-unsaturated bond for Michael addition reactions, such as thiol addition at C3, is strongly enhanced by the proximity of the electron-withdrawing C4-OH and C1-carbonyl groups.

Aldehydes such as hexanal (HA), *trans*-2-octenal (t2OE), *trans*-2-nonenal (t2NE), and malondialdehyde (MDA) have been shown to be oxidized by either class 1 or class 3 ALDH [5,10] in vitro, but it was not known whether this could protect against the toxic effects of these aldehydes in living cells. Stably transfected V79 cell lines previously developed in this laboratory that express either human

class 1 or class 3 ALDH [11,12] were utilized to examine whether ALDH expression is sufficient to confer resistance to specific toxic aldehydes. This transgenic model system facilitated comparison of cells that differ only in expression of ALDH isozymes, or lack thereof in the empty vector-transfected control line.

Acrolein is a short (3-carbon) α,β-unsaturated aldehyde that is a ubiquitous evironmental contaminant generated during oxidation of wood, tobacco, hydrocarbons, fats, etc. and also formed endogenously via metabolism of spermine and the important anticancer drug cyclophosphamide [13,14]. We have shown that acrolein can enhance cyclophosphamide toxicity in part via rapid depletion of GSH pools, and can also partially reverse the cellular resistance to this class of drugs that is due to expression of ALDH1A1 or ALDH3A1 [15]. In the course of these studies, we found that acrolein is a substrate of ALDH3A1 (but not ALDH1A1), with minimal substrate inhibition in the presence of physiological levels of the NAD^+ cofactor; in contrast, the GSH or MESNA conjugates of acrolein were oxidized by ALDH1A1 (but not by ALDH3A1) [15]. This observation led to the question of whether either ALDH would protect against the cytotoxic effects of acrolein. In addition, we have tested for the possibility of protection by ALDH against chloroacetaldehyde, another metabolic by-product of cyclophosphamide and ifosfamide. Last, the common and rapidly oxidized ALDH3A1 substrate benzaldehyde was also tested.

The results presented herein support a protective physiological role for human ALDH3A1 as a detoxifying enzyme that oxidizes medium chain-length lipid aldehydes (but not acrolein or chloroacetaldehyde). However, class 1 ALDH was found to have a very limited ability to protect from any of the lipid aldehydes tested. Detoxification of these aldehydes by class 3 ALDH has thus been shown in these studies to protect cells from a variety of effects including GSH depletion, protein alkylation, growth inhibition, cytotoxicity, and apoptosis.

2. Materials and methods

2.1. Materials

Trans-2-hexenal, *trans*-2-octenal, *trans*-2-nonenal, *n*-hexanal, acrolein, allylamine, acetaldehyde, chloroacetaldehyde, and benzaldehyde were obtained from Sigma or Aldrich Chemical Co. Malondialdehyde was prepared by acid hydrolysis of malondialdehyde bis(diethyl acetal) (Sigma) as previously described [16]. HNE was a gift of Dr Maryanne Hayn (University of Graz, Austria).

2.2. Cell lines and culture

Cells were grown in DMEM medium with 10% fetal bovine serum (GIBCO) at 37°C in a 5% CO_2 atmosphere. Chinese hamster lung fibroblast cells (V79) expressing rat cytochrome P450 2B1 (V79MZr2B1) were previously stably transfected with human ALDH expression vectors [11,12], and clones hALDH1-28

(expressing hALDH-1) and hALDH3-26 (expressing hALDH-3) were compared with the empty vector-transfected clone (Hyg-1) in these experiments. Similarly, analogous cell lines that stably express ALDH3A1, and an empty vector-transfected, non-expressing control line were established by stable transfection of the RAW 264.7 murine macrophage cell line [17].

2.3. ALDH activity analysis

Cells were lysed by brief sonication at 4°C in 50 mM Tris–HCl, pH 7.4, with 5 mM EDTA, lysates were centrifuged at 14 000*g* for 5 min at 4°C, and the supernatants were utilized for determining enzyme activity. Protein was determined by the bicinchoninic acid method (Pierce Chemical Co.). Enzyme activity was determined as previously described [12,18].

2.4. Growth inhibition analysis

Cells were plated (5×10^4/25 cm^2 flask) 24 h prior to aldehyde treatment in 10 mM HEPES-buffered DMEM plus 5% fetal bovine serum. The following day aldehyde stocks were diluted into 5 ml of medium and the flasks tightly capped and returned to the incubator for 48 h. In the case of acrolein and allylamine, the exposure period was 20 min in serum-free medium, to avoid complications due to the reaction of acrolein with serum proteins, and to favor activation of allylamine to acrolein by intracellular amine oxidases, rather than by extracellular amine oxidases present in serum [19]. The IC_{50} for growth inhibition was the concentration of aldehyde that reduced the increase in cell number by 50% after 48 h of growth.

2.5. Glutathione depletion assay

GSH was assayed by the GSSG-reductase/DTNB recycling method [20]. Samples of 3×10^6 cells were treated with lipid aldehydes in 100 mm^2 dishes for 30 min at 37°C in serum-free medium, lysed in 2% sulfosalicylic acid on ice for 5 min, and centrifuged 12 000*g*, 10 min at 4°C. Aliquots of the supernatant were assayed for total GSH + GSSG relative to a GSH standard curve.

2.6. Apoptosis assay

Cells were plated at 2×10^6 cells per 60 mm dish. After 16–20 h cells were rinsed and treated with agents in serum-free DMEM. After a 1 h exposure, medium was removed and replaced with DMEM + 10% fetal bovine serum. Cells were allowed to incubate for an additional 9 h at which time they were harvested in PBS and the DNA purified and analyzed for internucleosomal fragmentation by agarose gel electrophoresis as described [17].

2.7. HNE protein adduct detection

Control or ALDH-transfected V79 cells were plated at 2.5×10^6 cells/60mm dish and 16–20 h later cells were exposed to HNE for 1 h in serum-free medium. FBS was added to 10% at 1 h and cells were allowed to incubate for an additional hour. Cells were harvested and cytosolic protein (14 000 × *g* supernatant, 50 μg/lane) was electrophoresed, transferred by semi-dry electroblotting to nitrocellulose, probed using an anti–HNE/protein adduct antibody [21] and detected by chemiluminescence [17]. The scanned film was analyzed using NIH image, and areas under the plots of grayscale intensity were used as arbitrary units to estimate relative protein adduct formation detected in each lane.

3. Results

3.1. Protection against toxicity of medium-chain aliphatic aldehydes

Assays utilizing cytosol from the hALDH3-26 and hALDH1-28 cell lines, expressing high ALDH3A1 and ALDH1A1 respectively, indicated that the six- to nine-carbon aldehydes were excellent substrates for ALDH3A1, with specific activities ranging from 2000 to 8300 nmol/min/mg, but weak substrates for ALDH1A1 (all were around 7 nmol/min/mg). However, MDA was a rather poor substrate for both ALDH isozymes (12 and 6 nmol/min/mg, respectively). The growth inhibition assays (Fig. 1) demonstrated that ALDH3A1 conferred nine-fold protection against the toxicity of the saturated aldehyde hexanal, and 21-fold against toxicity of the α,β-unsaturated aldehyde trans-2-hexenal (t2HE) (Fig. 1A and B). Protection by ALDH3A1 against t2OE was 28-fold, while it reduced t2NE toxicity by 18-fold (Fig. 1C and D). Expression of ALDH1A1 conferred two-fold protection against t2HE, and five-fold protection against t2NE (Fig. 1B and D). The ALDH1A1 gave better protection (two-fold) only against MDA, against which ALDH3A1 was completely ineffective (Fig. 2). The fold-resistance to toxicity conferred by ALDH3A1 was relatively well-correlated with the substrate efficacy of these aldehydes, with a correlation coefficient of 0.8 (Fig. 3). Analysis of glutathione pools in cells exposed to t2OE and t2NE indicated that only ALDH3A1 expression protected against exhaustion of this critical antioxidant buffer system, which is known to be depleted by the α,β-unsaturated aldehydes in particular [9]. At concentrations of t2OE or t2NE that acutely depleted GSH more than 90% in the control Hyg-1 cells, hALDH3-26 cells exhibited only 20–30% GSH depletion, while the hALDH1-28 cells were depleted to the same degree as the control Hyg-1 cell line (data not shown).

3.2. Protection by ALDH3A1 against toxicity, protein alkylation, and apoptosis induced by HNE

The contributions of the component functional groups of HNE to potency of

induction of growth inhibition and apoptosis were determined in a structure–activity study [17]. The rank order of effects on toxicity to RAW 264.7 murine macrophage cells was C1–aldehyde $\geq$ C2 = C3 double bond > > C4–hydroxyl, with similar results in both the growth inhibition and apoptosis assays. Comparison of the closely related congener *trans*–2-nonenal to 2-nonenoic acid indicated IC_{50} values in the growth inhibition assay of 24 ± 4.3 μM and 1770 ± 342 μM respectively, or a 74-fold decrease in toxicity due to oxidation of the α,β-unsaturated aldehyde ([17]; not shown). Similarly, studies comparing non-expressing control V79 cells to the transfectant line expressing ALDH3A1 (which oxidizes HNE to 4-hydroxynonenoic acid) [17] showed 21-fold resistance to HNE toxicity in the hALDH3-26 cell line (not shown). Western blot analysis of HNE-protein covalent adducts indicated complete prevention of adducts by ALDH3A1, while expression of ALDH1A1 only raised the threshold by preventing adducts at low HNE

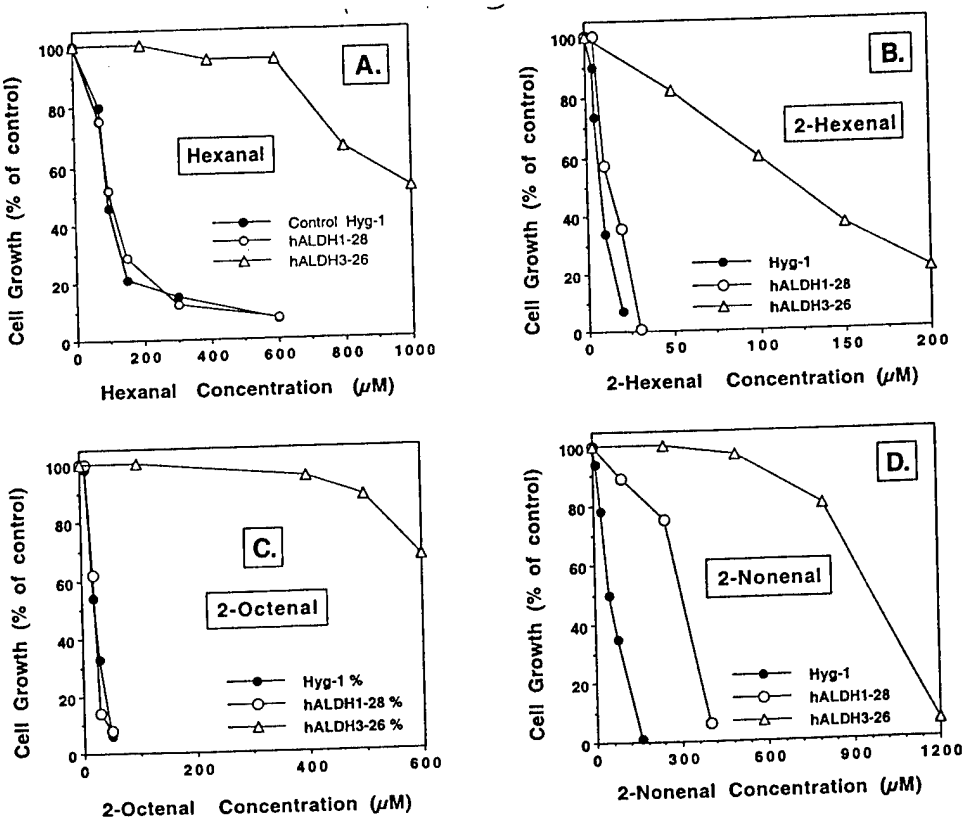

Fig. 1. Sensitivity of ALDH-transfected V79 cell lines to growth inhibition by medium-chain lipid aldehydes. Cells (5×10^4) were treated with aldehydes as indicated for 48 h, then counted as described in Section 2.4. Results are expressed as the percent of the growth over 48 h in each cell line treated with vehicle only. Each panel represents the average of two or more experiments.

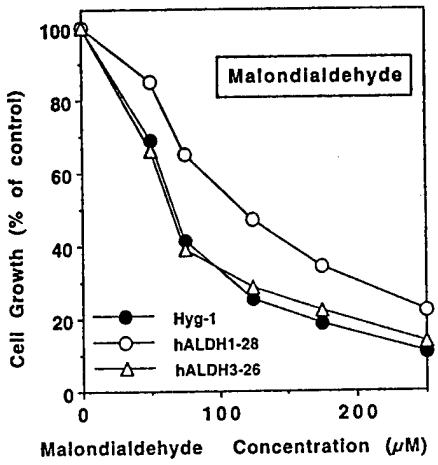

Fig. 2. Sensitivity of ALDH-transfected V79 cell lines to growth inhibition by malondialdehyde. Cells were plated and treated with malondialdehyde as described in Fig. 1, harvested, and counted as described in Section 2.4. Results represent the average of two or more experiments.

concentrations (Fig. 4). Similar results were obtained in the RAW 264.7 cells expressing ALDH3A1; furthermore, the HNE-induced apoptosis was completely prevented in the ALDH3A1-transfected RAW264.7 line up to 70 μM HNE [17] (not shown).

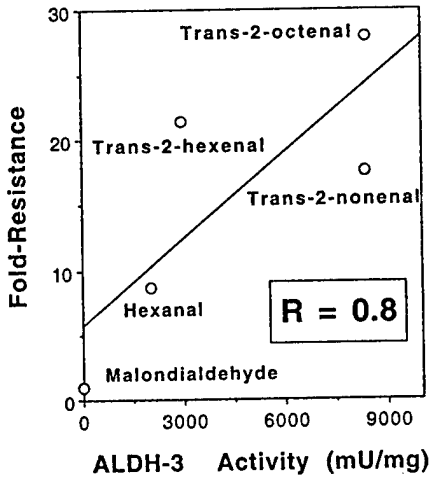

Fig. 3. Correlation between specific activity with ALDH3A1 and resistance to toxicity for a range of aliphatic aldehydes. The specific activity was determined for each substrate with cytosolic protein from V79 cells expressing ALDH3A1, and the result plotted against the fold-resistance to the toxicity of each (IC_{50} of the hALDH3-expressing line divided by the IC_{50} of the non-expressing line). The best-fit line was determined and correlation coefficient calculated by the method of least squares.

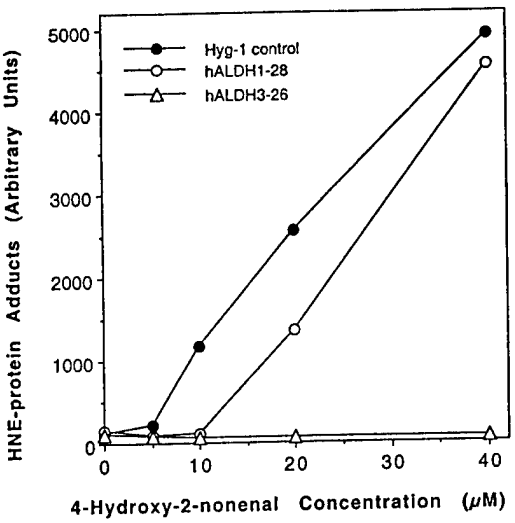

Fig. 4. Prevention of protein adducts formed in cells treated with 4-hydroxy-2-nonenal by ALDH3A1 expression. Cells were plated at 2.5×10^6 cells/60mm dish and exposed to HNE for 1 h in serum-free medium, then processed and protein adducts detected by immunoblot analysis using antisera directed against HNE adducts, and the blot was analyzed by densitometry as described in Section 2.7 and Ref. [17]. The baseline-corrected total area under the plot of grayscale density for each entire lane was plotted as total adducts formed (arbitrary units) at each concentration of HNE.

3.3. Lack of protection by ALDH against acrolein, chloroacetaldehyde, or benzaldehyde

The generation of acrolein and chloroacetaldehyde during metabolism of cyclophosphamide, together with our previously published evidence that low concentrations of acrolein increased the drug sensitivity of both control and ALDH-expressing cell lines [15], suggested the possibility that ALDH expression might directly protect against acrolein toxicity. Acrolein is oxidized by ALDH3A1, while its GSH conjugate is oxidized by ALDH1A1 [15,22]. However, expression of either of these isozymes failed to confer any resistance to acrolein (Fig. 5A). Because acrolein is so reactive, we reasoned that it may preferentially damage membrane proteins to a lethal extent before a major portion can be detoxified by ALDH in the cytosolic compartment. We therefore repeated the experiments with allylamine, a compound that is converted to acrolein by intracellular amine oxidase activity [18]. The IC_{50} values were increased ten-fold for all cell lines, presumably due to the requirement for metabolic activation; however, there was no protection by either ALDH isozyme against allylamine (Fig. 5B). Similarly, both ALDH isozymes failed to confer resistance to either chloroacetaldehyde or the ethanol metabolite acetaldehyde with either long (24 h; Fig. 6) or short exposures (20 min; not shown). The failure of ALDH1A1 to protect against the weakly toxic substrate acetaldehyde, even at high concentrations required to kill the cells that are in the catalytic range of this enzyme, might be attributable to the low turnover of this

substrate. We therefore tested whether ALDH3A1 would protect against benzaldehyde, a substrate that is also weakly toxic but has a much higher turnover rate. Surprisingly, while expression of ALDH1A1 had no effect on sensitivity, the expression of ALDH3A1 resulted in approximately two-fold sensitization to the growth inhibitory effects of benzaldehyde (Fig. 7).

4. Discussion

Expression of class 3 aldehyde dehydrogenase activity has been proposed as a defensive mechanism against toxic lipid aldehydes generated during LPO [10]. Consistent with this view, the results of these growth inhibition studies demonstrated that ALDH3A1 protected well against the growth-inhibitory effects of medium chain-length aliphatic aldehydes produced during LPO. Comparison of the relative protection against hexanal versus trans-2-hexenal (Fig. 1 A and B), and nonanal versus *trans*-2-nonenal [17] clearly indicated that protection was more efficacious against the α,β-unsaturated aldehydes. This is not surprising, considering that the latter have two reactive sites, the aldehyde and the Michael addition site at C3, that interact in a synergistic fashion due to mutual enhancement of reactivity between the carbonyl and the double bond. This was confirmed by the 14-fold greater toxicity of *trans*–2-nonenal than the saturated analog nonanal, and 74-fold greater toxicity than 2-nonenoic acid, which lacks the aldehyde [17]. A portion of

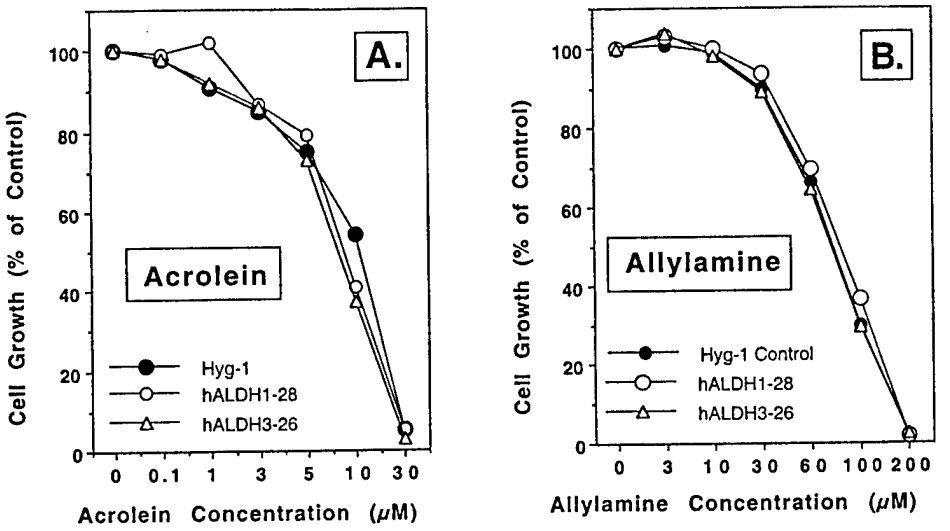

Fig. 5. Sensitivity of ALDH-transfected V79 cell lines to growth inhibition by acrolein or allylamine. Cells (5×10^4) were treated with aldehydes as indicated for 20 min, then grown for 48 h and counted as described in Section 2.4. Results are expressed as the percent of the growth in each cell line treated with vehicle only. Results with allylamine are the average of three experiments; results with acrolein are from a single experiment (similar results with 24 h exposures).

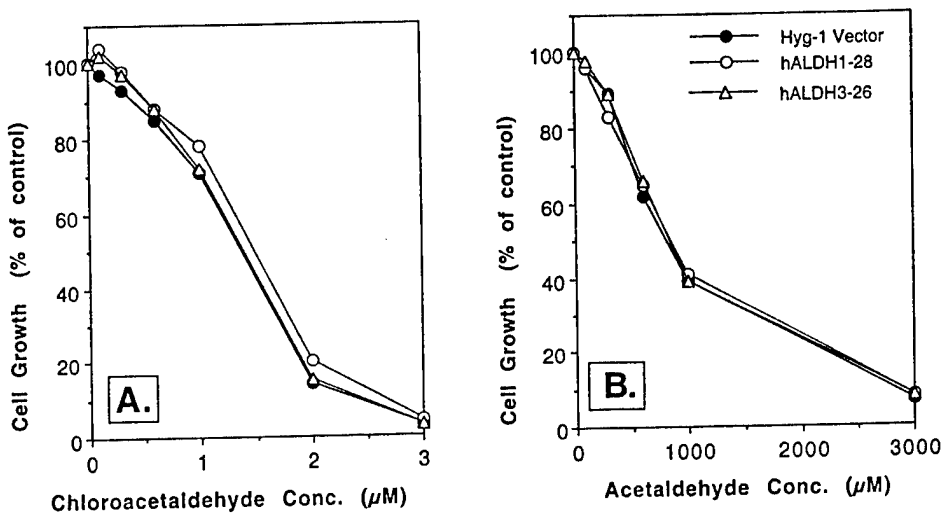

Fig. 6. Sensitivity of ALDH-transfected V79 cell lines to growth inhibition by chloroacetaldehyde or acetaldehyde. Cells (5×10^4) were treated with aldehydes as indicated for 48 h and counted as described in Section 2.4. Results are expressed as the percent of the growth in each cell line treated with vehicle only. Results are the average of two experiments.

the protection against aliphatic aldehyde toxicity may be attributable to the partial reversal by ALDH3A1 of their ability to deplete GSH. We also found that ALDH3A1, but not ALDH1A1 reversed the DNA synthesis inhibition by these same aldehydes (not shown).

Although MDA is a far more abundant aldehyde product of LPO, it was ten-fold less potent than HNE in its growth inhibitory effects. We found only weak protection against MDA toxicity by ALDH1A1, and none by ALDH3A1. Conversely, however, potent protection was observed against HNE toxicity, protein adduct formation, inhibition of macromolecular synthesis (not shown) and induction of apoptosis in both V79 and RAW 264.7 cells expressing ALDH3A1, while only slight protection was conferred by ALDH1A1 expression. A fundamental mechanism of protection against HNE toxicity and apoptosis appears to be the complete prevention by ALDH3A1 expression of the extensive protein adduct formation observed when control cells were exposed to HNE [17].

The failure of either ALDH3A1 or ALDH1A1 to protect against the toxicity of acrolein may be due to several factors. We have previously shown that ALDH3A1 is at least partially protected from irreversible inhibition by acrolein in the presence of NAD^+ at concentrations present in cells [15]. We tested allylamine, which is activated by intracellular amine oxidases, to test the possibility that acrolein is so reactive that it kills cells by becoming covalently bound primarily to surface proteins, which cannot be prevented by detoxification mechanisms in the cytosol. However, although the IC_{50} was ten-fold higher due to the activation step, again there was no protection by either ALDH. Thus the most straightforward explana-

tion is simply inadequate activities for oxidation of the aldehyde group of acrolein or its GSH conjugate by ALDH3A1 or ALDH1A1, respectively [15].

There was also no protection by either ALDH against chloroacetaldehyde, a byproduct of metabolic activation of cyclophosphamide and ifosfamide, and a putative cause of their neurotoxic side effects. Acetaldehyde was also tested, since it is much less reactive and far less toxic, and hence has an IC_{50} that is in the catalytic range of ALDH1A1; however, it was also equally toxic to all cell lines regardless of whether ALDH was expressed. Since the failure to protect against any of these small aldehyde substrates could potentially be due simply to catalytic inefficiency, we also examined efficacy against growth inhibition by benzaldehyde, which is an excellent substrate for ALDH3A1 in the millimolar range, where toxicity also occurs. Surprisingly, the cells expressing ALDH3A1 were slightly (two-fold) more sensitive than either the control line or the ALDH1A1 expressing line, which had identical sensitivities. The substrate efficacy of benzaldehyde might cause a major shift in the stoichiometry of the NAD^+/NADH redox couple (normally > 50:1) such that the intracellular redox potential is excessively reducing, rather than oxidizing as in unstressed cells. Another possible explanation could be that the oxidized product of ALDH3A1 catalysis, benzoic acid, which is ionized at physiological pH, may be poorly transported out of cells and may accumulate to toxic levels during the exposure period. Cytotoxicity of accumulated GSH conjugates has been proposed as partial explanation for the requirement that a conjugate efflux mechanism be present in order to enable full protection against certain agents

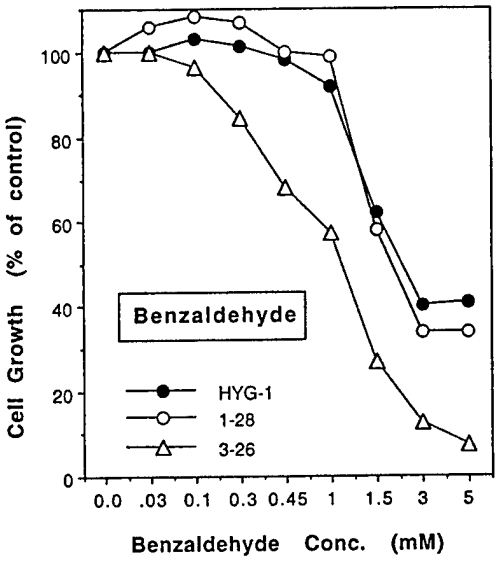

Fig. 7. Sensitivity of ALDH-transfected V79 cell lines to growth inhibition by benzaldehyde. Cells (5×10^4) were treated with benzaldehyde as indicated for 48 h and counted as described in Section 2.4. Results are expressed as the percent of the growth in each cell line treated with vehicle only. Results are the average of three or more experiments.

that are substrates for glutathione *S*-transferases (GSTs), e.g. 4-nitroquinoline-1-oxide and 4-Cl-2,4-dinitrobenzene [23,24]. Indeed, we have also observed that expression in V79 cells of mGSTA4, by far the most active murine GST isozyme for conjugation of HNE, not only fails to protect against cytotoxicity, in fact it actually renders cells slightly more sensitive to HNE (R. Haynes and A. Townsend, unpublished results). The possibility remains, however, that co-expression of GST and an energy-dependent conjugate efflux transporter in the multidrug resistance protein family (e.g. MRP1 or MRP2) may confer HNE resistance.

In summary, we have shown that ALDH3A1, but not ALDH1A1, can confer strong resistance to the protein damage, GSH depletion, macromolecular synthesis inhibition, growth inhibition, and apoptosis induced by aldehydes produced during lipid peroxidation. The potential protective functions of other isozymes in the expanding family of ALDH genes, their transcriptional regulation, and the impact on ALDH protective efficacy of ancillary cellular factors such as thiol content, regulation of redox homeostasis, product transport, and regulation of apoptotic signalling pathways will be important to investigate as well.

Acknowledgements

Supported by NIH Grant CA-76283, and small grants from the Leukemia Research Foundation and Bristol-Myers Squibb, Inc. We wish to acknowledge the generous gift of the human ALDH1A1 cDNA from Dr Henry Weiner, Purdue University.

References

[1] H. Esterbauer, R.J. Schaur, H. Zollner, Chemistry and biochemistry of 4-hydroxynonenal, malonaldehyde and related aldehydes, Free Radic. Biol. Med. 11 (1991) 81–128.
[2] B. Halliwell, J. Gutteridge, Lipid peroxidation: a radical chain reaction, in: Free Radicals in Biology and Medicine, Clarendon Press, Oxford, MA, 1985, pp. 139–189.
[3] P. Marshall, Role of active oxygen in the formation of lipid hydroperoxides, in: W. Lands (Ed.), Biochemistry of arachidonic acid metabolism, Martinus Nijhoff Publishing, Boston, MA, 1985, pp. 97–117.
[4] C. Vaca, J. Wilhelm, M. Harms-Ringdahl, Interaction of lipid peroxidation products with DNA. A review, Mut. Res. 195 (1988) 137–149.
[5] R. Lindahl, Aldehyde dehydrogenases and their role in carcinogenesis, Crit. Rev. Biochem. Mol. Biol. 27 (1992) 283–335.
[6] A. Benedetti, M. Comporti, H. Esterbauer, Identification of 4-hydroxynonenal as a cytotoxic product originating from the peroxidation of liver microsomal lipids, Biochem. Biophys. Acta 620 (1980) 281–296.
[7] R. Canonero, A. Martelli, U.M. Marinari, G. Brambilla, Mutation induction in Chinese hamster lung V79 cells by five alk-2-enals produced by lipid peroxidation, Mut. Res. Lett. 244 (1990) 153–156.
[8] H. Esterbauer, Cytotoxicity and genotoxicity of lipid-oxidation products. [Review], Am. J. Clin. Nut. 57 (1993) 779S–785S.
[9] G.. Witz, Biological interactions of alpha,beta-unsaturated aldehydes. [Review] [114 refs], Free Radic. Biol. Med. 7 (1989) 333–349.

[10] R. Lindahl, D.R. Petersen, Lipid aldehyde oxidation as a physiological role for class 3 aldehyde dehydrogenases, Biochem. Pharmacol. 41 (1991) 1583–1587.
[11] K.D. Bunting, A.J. Townsend, De novo expression of transfected human class 1 aldehyde dehydrogenase (ALDH) causes resistance to oxazaphosphorine anti-cancer alkylating agents in hamster V79 cell lines, J. Biol. Chem. 271 (1996) 11884–11890.
[12] K.D. Bunting, A.J. Townsend, Protection by transfected rat or human class 3 aldehyde dehydrogenases against the cytotoxic effects of oxazaphosphorine alkylating agents in hamster V79 cell lines-Demonstration of aldophosphamide metabolism by the human cytosolic class 3 isozyme, J. Biol. Chem. 271 (1996) 11891–11896.
[13] C. Izard, C. Lieberman, Acrolein, Mut. Res. 47 (1978) 115–138.
[14] N.E. Sladek, Metabolism of oxazaphosphorines, Pharmacol. Ther. 37 (1988) 301–355.
[15] K.D. Bunting, A.J. Townsend, Dependence of aldehyde dehydrogenase-mediated oxazaphosphorine resistance on soluble thiols: importance of thiol interactions with the secondary metabolite acrolein, Biochem. Pharmacol. 56 (1998) 31–39.
[16] R. Recknagel, A. Ghoshal, New data on the question of lipoperoxidation in carbon tetrachloride poisoning, Exp. Mol. Pathol. 5 (1966) 108–117.
[17] Haynes, R., Szweda, L., Pickin, K., Welker, M., Townsend, A. Structure–activity relationships for growth inhibition and induction of apoptosis by 4-hydroxy 2-nonenal in raw 264.7 cells. Mol. Pharmacol., (in press).
[18] C.L. Manthey, N.E. Sladek, Kinetic characterization of the catalysis of 'activated' cyclophosphamide (4-hydroxycyclophosphamide/aldophosphamide) by mouse hepatic aldehyde dehydrogenases, Biochem. Pharmacol. 37 (1988) 2781–2790.
[19] D.J. Conklin, S.D. Langford, P.J. Boor, Contribution of serum and cellular semicarbazide-sensitive amine oxidase to amine metabolism and cardiovascular toxicity, Toxicol. Sci. 46 (1998) 386–392.
[20] F. Tietze, Enzymic method for quantitative determination of nanogram amounts of total and oxidized glutathione, Anal. Biochem. 27 (1969) 502–522.
[21] J.A. Cohn, L. Tsai, B. Friguet, L.I. Szweda, Chemical characterization of a protein-4-hydroxy-2-nonenal cross-link: immunochemical detection in mitochondria exposed to oxidative stress, Arch. Biochem. Biophys. 328 (1996) 158–164.
[22] D. Mitchell, D. Petersen, Metabolism of the glutathione-acrolein adduct, *S*-(2-aldehydoethyl)glutathione, by rat liver alcohol and aldehyde dehydrogenase, J. Pharmacol. Exp. Ther. 251 (1989) 193–198.
[23] S.K. Diah, P.K. Smitherman, A.J. Townsend, C.S. Morrow, Detoxification of 1-chloro-2,4-dinitrobenzene in MCF7 breast cancer cells expressing glutathione *S*-transferase P1-1 (GSTP1-1) and/or multidrug resistance protein 1 (MRP1), Toxicol. Appl. Pharmacol. 157 (1999) 85–93.
[24] C.S. Morrow, S. Diah, P.K. Smitherman, E. Schneider, A.J. Townsend, Multidrug resistance protein and glutathione *S*-transferase P1-1 act in synergy to confer protection from 4-nitroquinoline 1-oxide toxicity, Carcinogenesis 19 (1998) 109–115.

Free Radical Biology & Medicine, Vol. 30, No. 8, pp. 884–894, 2001

0891-5849/01/$–see front matter

ELSEVIER

PII S0891-5849(01)00476-2

Original Contribution

APOPTOSIS IN RAW 264.7 CELLS EXPOSED TO 4-HYDROXY-2-NONENAL: DEPENDENCE ON CYTOCHROME *C* RELEASE BUT NOT P53 ACCUMULATION

ROBIN L. HAYNES,* BERNARD BRUNE,† and ALAN J. TOWNSEND*

*Department of Biochemistry, Wake Forest University School of Medicine and Comprehensive Cancer Center of Wake Forest University, Winston Salem, NC, USA; and †University of Erlangen-Nürnberg, Department of Medicine IV, Experimental Division, Erlangen, Germany

(*Received* 6 *November* 2000; *Revised* 12 *January* 2001; *Accepted* 16 *January* 2001)

Abstract—The toxic reactive aldehyde lipid peroxidation byproduct 4-hydroxy-2-nonenal (HNE) is thought to be a major contributor to oxidant stress-mediated cell injury. HNE induced apoptosis in RAW 264.7 murine macrophage cells in a dose-dependent manner within 6–8 h after exposure. Expression of the antiapoptotic protein Bcl-2 in stably transfected RAW 264.7 cells prevented HNE-induced internucleosomal DNA fragmentation and apoptosis, and these cells resume growth after a temporary (24–48 h) growth delay. While parental RAW 264.7 cells released mitochondrial cytochrome *c* within 3 h after HNE exposure, expression of Bcl-2 prevented cytochrome *c* release. In control cells, p53 protein levels peaked at 6–9 h after HNE exposure and then declined, while in Bcl-2 expressing cells, p53 levels were maximal at 6–9 h and remained elevated up to 96 h. Expression of SV40 large T-antigen, which forms a stable complex with p53 protein, via stable transfection-blocked transactivation of the p53-regulated gene $p21^{WAF1/CIP1}$, but did not affect induction of apoptosis by HNE, suggesting that p53 function is not important in HNE-induced apoptosis. These results suggest that cytochrome *c* release, but not p53 accumulation, plays an essential role in HNE-induced apoptosis in RAW 264.7 cells. © 2001 Elsevier Science Inc.

Keywords—4-hydroxy-2-nonenal, Apoptosis, P53 tumor suppressor, Cytochrome *c*, Bcl-2, $P21^{WAF1/CIP1}$, SV-40 T-antigen, Lipid peroxidation, DNA fragmentation, Free radicals

INTRODUCTION

Oxidative stress, defined as cellular damage due to an excess of pro-oxidant species relative to antioxidant defensive capacity, involves the production of reactive oxygen species (ROS) that can damage protein, DNA, and membranes. For example, ROS can originate from inflammatory processes, exposure to UV, oxidant-producing chemicals, mitochondrial dysfunction, and general oxidative metabolism in cells with low antioxidant defenses. Potentially one of the most damaging effects of ROS production is initiation of lipid peroxidation, a radical-mediated chain reaction that occurs when ROS oxidize cellular membrane lipids [1].

Polyunsaturated fatty acids such as arachidonic acid interact with ROS and a radical-mediated chain reaction occurs that weakens membrane integrity and produces a series of toxic byproducts including radical species, alcohols, aldehydes, and lipid hydroperoxides. While some of these species are highly reactive but short-lived, certain lipid aldehyde products such as 4-hydroxy-2-nonenal (HNE) remain stable in the lipid bilayer and subsequently diffuse into the cytosol from the site of production in the membrane. The strong reactivity of HNE derives from the interaction of the electronegative 1-carbonyl and the 4-hydroxyl groups with the C2=C3 double bond, rendering this electrophilic site highly susceptible to nucleophilic attack, e.g., by thiolate anion in GSH or proteins [2]. It has been estimated that localized HNE concentrations can increase to as high as 4.5 mM within peroxidizing membrane bilayers [1]. Thus, although other aldehydes are produced in higher abundance during lipid peroxidation, the reactivity of HNE makes it one of the most potentially dangerous products of oxidative stress.

Address correspondence to: Dr. Alan J. Townsend, Wake Forest University School of Medicine, Biochemistry Department, Medical Center Boulevard, Winston-Salem, NC 27157, USA; Tel: (336) 716-7658; Fax: (336) 716-7671; E-Mail: atown@wfubmc.edu.

HNE is known to cause a number of deleterious effects in cells including glutathione depletion [3], DNA and RNA synthesis inhibition [4], calcium homeostasis disturbances [5], and inhibition of mitochondrial respiration [6]. In addition, HNE has been reported to activate signaling via c-Jun N-terminal kinase, and to inhibit other regulatory mechanisms such as NF-κB and the proteasomal degradation pathway [7–9]. Recently HNE has been shown to induce apoptosis in certain cell lines [10,11]. We have characterized the structure-activity relationships of HNE functional groups in regard to apoptosis induction potency in RAW 264.7 cells [12]. Both oxidant stress-induced apoptosis and HNE-protein adducts have been found in tissues in association with ischemia-reperfusion injury, neurodegenerative disorders, and autoimmune diseases [13]. This suggests etiologic causality between induction of apoptosis by oxidant stress-generated lipid peroxidation byproducts and the pathological states in these and related disease processes, and highlights the importance of understanding the basic mechanisms involved in HNE-induced apoptosis. We have investigated the potential contributions to HNE-induced apoptosis of two pathways frequently linked to apoptotic signaling, the first mediated by tumor suppressor protein p53 and the second involving the release of the mitochondrial inner-membrane protein cytochrome *c*.

The p53-mediated and mitochondria-mediated pathways are two key mechanisms involved in induction of apoptosis, with apparent convergence in the late stages due to recruitment of mitochondria involvement downstream of p53 signaling. Numerous studies have shown participation of p53 in apoptotic responses to DNA damage caused by UV exposure [14,15], gamma radiation [16,17], chemical carcinogenesis, and chemotherapeutic drugs [18,19]. Upon sensing DNA damage p53 becomes phoshorylated by kinases, stabilizing and activating the normally short-lived protein [20–22]. Stabilized p53 transactivates transcription of downstream effectors such as $p21^{WAF1/CIP1}$, BAX, and GADD45 [23–25]. These molecules respond by affecting either cell cycle, apoptotic cell death, or DNA repair, respectively. After the response is transduced, p53 is degraded through MDM2-targeted ubiquitin-mediated proteolysis [26,27]. P53 can be inhibited by interaction with molecules such as SV40 large T-antigen, which binds p53 and prevents downstream function [28,29].

Induction of apoptosis by the mitochondrial pathway may result from depolarization of inner membrane ionic potential ("permeability transition") due to direct damage or opening of a high-conductance pore as a result of signal transduction as an early primary event [30,31]. Release of the electron transport protein cytochrome *c*, presumably the result of mitochondrial swelling and transient rupture of the outer membrane, initiates downstream cascades of caspase activation, DNA fragmentation, morphological changes, and finally vesicular partitioning [32]. Antiapoptotic proteins such as Bcl-2 are thought to act at the level of the mitochondria by inhibiting the release of cytochrome *c*, thus protecting the cell from apoptosis [33]. The results presented herein indicate that induction of apoptosis by HNE is correlated with cytochrome *c* release that is blocked by Bcl-2, but does not appear to be dependent on p53 function.

MATERIALS AND METHODS

Cell culture and reagents

Mouse alveolar macrophage RAW 264.7 cells were grown at 37°C in a 5% CO2 atmosphere in DMEM medium (Gibco; Grand Island, NY, USA) supplemented with 10% fetal bovine serum (FBS). Derivation of the Bcl-2-transfected RAW 264.7 cell line (clone 14) has been previously described [34]. 4-Hydroxynonenal was purchased from Cayman Chemical (Ann Arbor, MI, USA). Proteinase K was purchased from Promega (Madison, WI, USA). Digitonin was purchased from Fluka Chemical (Milwaukee, WI, USA). All other chemicals were purchased from Sigma Chemical Co. (St. Louis, MO, USA).

HNE protein adduct detection

Cells were plated at 2.5×10^6 cells/60 mm dish and 16–20 h later cells were exposed to agents for 1 h in serum-free medium. FBS was added to 10% at 1 h and cells were allowed to incubate for an additional hour. Cells were harvested by scraping into cold phosphate-buffered saline (PBS), centrifuged at $500 \times g$, and the pellets lysed by brief sonication in 50 mM Tris, 5 mM EDTA, and 1 mM PMSF. Lysates were centrifuged at $14{,}000 \times g$ for 10 min at 4°C and protein (50 μg/lane) was electrophoresed on a 10% SDS-PAGE gel and transferred to nitrocellulose. Adducts were detected using an anti-HNE-protein adduct antibody [35] kindly provided by Dr. Luke Szweda (Case Western Reserve University; Cleveland, OH, USA) at a dilution of 1:2500. After probing with goat anti-rabbit, horseradish peroxidase-conjugated secondary antibody (Biorad; Hercules, CA, USA) (1:3000), the HNE-modified protein was detected using Renaissance chemiluminescence reagent (NEN Life Science Products; Boston, MA, USA).

DNA fragmentation

Cells were plated at 7×10^6 cells per 100 mm culture dish. After 16–20 h, cells were rinsed and treated for 1 h

in serum-free DMEM containing the indicated concentrations of HNE. After a 1 h exposure, medium was removed and replaced with DMEM + 10% fetal bovine serum. Cells were harvested at the indicated time by gently scraping into cold PBS and collected by centrifugation at 500 × *g* at 4°C for 5 min. One tenth of the collected cells was used for DNA fragmentation while the remaining cells were stored at −20°C for protein analysis. Cells for fragmentation analysis were lysed in 20 mM EDTA, 100 mM Tris (pH 8.0), 0.8% sodium lauryl sarcosine, and treated with RNase (0.5 mg/ml) for 2 h at 37°C. Lysates were then treated with proteinase K (5 mg/ml) for 6–12 h at 55°C. DNA content was quantitated in each lysate sample by absorbance at 260 nm and sample concentrations were adjusted and normalized to DNA content. Samples were processed and analyzed by electrophoresis on ethidium bromide stained 1.6% agarose gel as previously described [12].

Cytochrome c release

Cytochrome *c* release was assayed as previously described [36]. Briefly, cells were plated at 7×10^6 cells/100 mm dish. After 16–20 h, cells were exposed to HNE for 1 h in serum-free media. At the indicated times, cells were harvested by scraping into cold PBS and collected by centrifugation. Seventy percent of the cells were used for cytochrome *c* release while the remaining 30% were used for p53 stabilization studies. The cells for cytochrome *c* studies were resuspended in room temperature PBS. An equal volume of 500 mM sucrose containing 150 μM digitonin was added and the cells were vortexed for 10 s at low speed. After 30 s, cells were centrifuged for 4 min at 13,000 × *g* at 4°C. The supernatant was removed, supplemented with 1 mM PMSF, 0.5 μg/ml leupeptin, and 0.7 μg/ml pepstatin, and frozen at −80°C until all samples were collected.

For cytochrome *c* detection, cytosolic protein (50 μg) was electrophoresed on a 15% SDS-PAGE gel and transferred to nitocellulose by semidry electrophoresis. Cytochrome *c* was detected using an anti-cytochrome *c* monoclonal antibody clone 7H8.2C12 (PharMingen; San Diego, CA, USA) at 1 μg/ml. After probing with a goat anti-mouse, horseradish peroxidase-conjugated secondary antibody (Biorad) (1:3000 dilution in 1% nonfat milk) labeled bands were detected using chemiluminescence (NEN Life Science Products).

Transfection of SV40 large T-antigen

The plasmid pSVT#3 [37] encoding simian virus large T-antigen cDNA and a neomycin resistance gene was kindly provided by Dr. Sumitra Deb (Medical College of Virginia). This plasmid, or the control empty vector, neomycin resistance plasmid pRc/CMV (Invitrogen; Carlsbad, CA, USA) were transfected separately into RAW 264.7 parental cells with the cationic liposome reagent Escort (Sigma Chemical Co.). Briefly, cells were plated in 100 mm culture dishes and grown to 70–80% confluency. Escort (30–50 μl) was incubated with DNA (15–25 μg) in 800 μl of Opti-MEM transfection medium (Gibco) for 15 min. Opti-MEM was added to Escort/DNA mixture to a total volume of 8 ml. Cells were then allowed to incubate in transfection medium for 6 h. An equal volume of DMEM + 10% FBS was added and cells were incubated overnight. Cells were selected for neomycin resistance in selection media (DMEM/10% FBS plus 1.0 mg/ml G418 [Gibco]). Isolated colonies were expanded and screened for T-antigen protein expression using monoclonal antibody pAB 419 [38] (also provided by Dr. Sumitra Deb).

Western blot analysis for p53 studies and TAg overexpressing studies

Cells were plated at 7×10^6 cells/100 mm petri dish. After exposure to HNE, cells were collected and lysed in 50 mM Tris (pH 8.0), 5 mM EDTA, 150 mM NaCl, 0.5% NP40, 1 mM PMSF, 0.5 μg/ml leupeptin, and 0.7 μg/ml pepstatin. Lysates were centrifuged at 13,000 × *g* for 5 min (4°C) and 100 μg of supernatant protein was run on a 10% SDS-PAGE gel and transferred to nitrocellulose. P53 was detected using hybridoma supernatant pAB 122 [39] at a dilution of 1:100. TAg was detected using hydridoma supernatant pAB 419 at a dilution of 1:10. $P21^{WAF1/CIP1}$ was detected using monoclonal antibody anti- $p21^{WAF1/CIP1}$ clone SXM30 (PharMingen) at 1 μg/ml. For final detection, all blots were incubated with goat anti-mouse horseradish peroxidase-conjugated secondary antibody (Biorad) at a dilution of 1:3000 followed by chemiluminescence detection.

RESULTS

Expression of Bcl-2 blocks HNE-induced apoptosis but not protein adducts

The antiapoptotic protein Bcl-2 has been shown to stabilize mitochondria and prevent the release of cytochrome *c* into the cytosol. Therefore, a RAW 264.7 cell line expressing stably transfected Bcl-2 [34] was compared to the parental line to determine the importance of mitochondrial cytochrome *c* release in HNE-induced apoptosis. Although Bcl-2 expression in RAW 264.7 parental cells is undetectable by western blot analysis, a strong band was observed in the Bcl-2-14 transfected but otherwise isogenic cell line (Fig. 1).

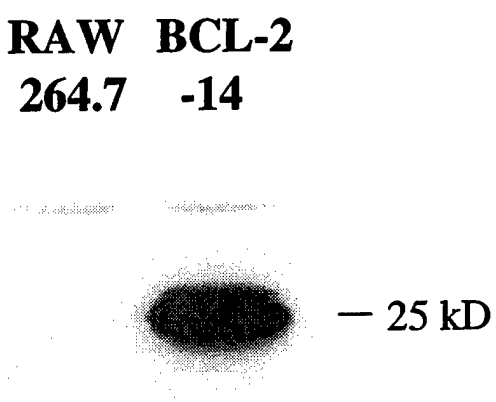

Fig. 1. Overexpression of Bcl-2. Total protein (50 μg/lane) from RAW 264.7 parental cells and RAW 264.7 cells transfected with human Bcl-2 (clone 14) was run on a 12% SDS-PAGE gel, transferred to nitrocellulose, and probed with polyclonal antibody Bcl-2 (N-19) (Santa Cruz Biotechnology; Santa Cruz, CA, USA) at a 1:300 dilution as described in Materials and Methods.

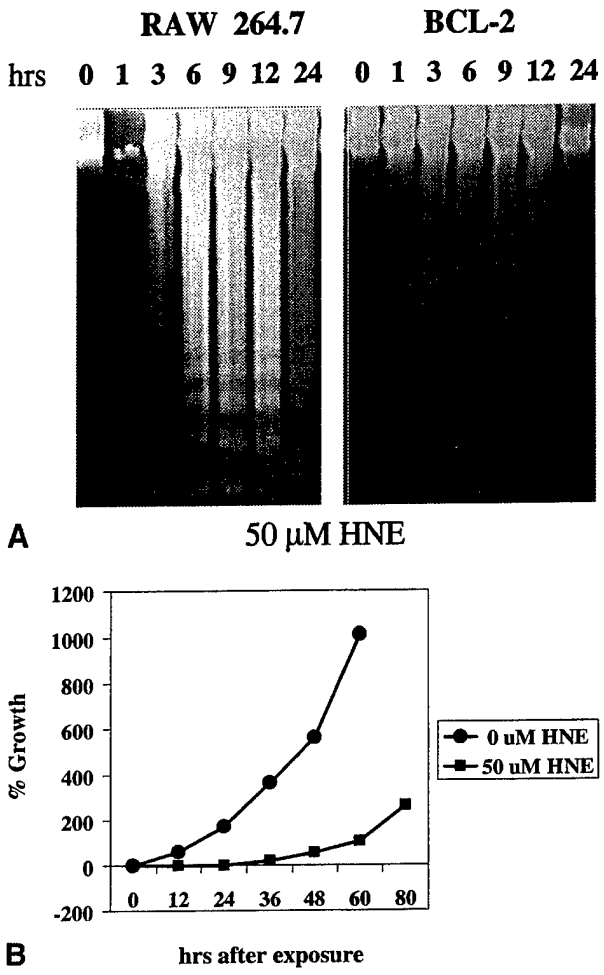

Fig. 2. (A) Bcl-2 expression protects against HNE-induced internucleosomal DNA fragmentation. RAW 264.7 parental cells and parental cells overexpressing Bcl-2 were exposed to 50 μM HNE for 1 h in serum-free media. Cells were harvested at the indicated times and DNA was isolated, electrophoresed, and stained with ethidium bromide as described in Materials and Methods. (B) HNE induces a temporary growth inhibition (up to 48 h) in Bcl-2-expressing cells. Bcl-2-expressing cells were exposed to either 0 or 50 μM HNE for 1 h in serum-free media. Cells were trypsinized and counted at the indicated times using a Coulter Cell counter (Coulter Corp.; Westbrook, ME, USA).

When RAW 264.7 cells were exposed to 50 μM HNE, apoptotic DNA fragmentation was detected as early as 3 h after exposure (Fig. 2A). Within 12 h after exposure, greater than 90% of the cells exhibited late stage morphological changes: apoptotic blebs and blisters (seen under time-lapse video microscopy; not shown). Also, initial cell viability was determined by trypan blue exclusion using increasing concentrations of HNE. Cells remained viable and membranes remained intact for 2–5 h (depending on HNE concentration) after the initial exposure to HNE concentrations up to 75 μM. This indicates that there was no direct membrane permeabilization due to the lipophilic nature of HNE. When Bcl-2 overexpressing cells were exposed to 50 μM HNE, no apoptotic DNA fragmentation was seen up to 24 h after the exposure (Fig. 2A), although they displayed a significant delay in growth when compared to untreated controls (Fig. 2B).

When the HNE concentration was increased to 75 μM, Bcl-2 overexpressing cells continued to show no apoptosis (shown in Fig. 7), but at higher concentrations a nonspecific degradation pattern characteristic of necrotic death was observed (not shown). At lower concentrations (below 25 μM), no apoptotic DNA fragmentation could be detected in either the parental or Bcl-2-expressing RAW 264.1 cells. However, both cell lines displayed a concentration-dependent growth inhibition at low, nonapoptotic HNE concentrations (data not shown). Measurement of HNE-protein adducts by immunoblotting showed that Bcl-2 overexpression did not protect against apoptosis by reducing overall adduct formation (Fig. 3). Therefore the antiapoptotic effects of Bcl-2 expression occur in subsequent steps of the cascade of apoptotic events, beyond initial protein modification by HNE.

HNE-induced p53 protein accumulation and cytochrome c release

Accumulation of p53 tumor suppressor and release of cytochrome *c* from the inner membrane space of the mitochondria into the cytosol have been implicated as mediators of oxidant stress-induced apoptosis. Therefore, p53 protein levels and release of cytochrome *c* were examined by immunoblotting over a period of 12 h. Both the appearance of cytochrome *c* in cytosolic fractions

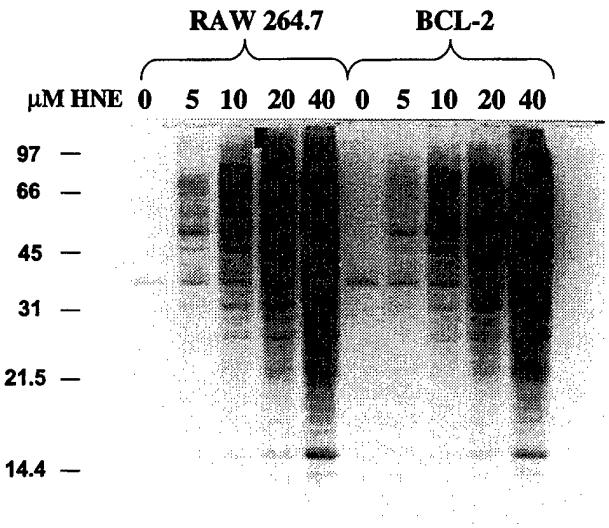

Fig. 3. Bcl-2 expression does not protect against HNE-induced protein adduct formation. Parental and Bcl-2-expressing cells were exposed to increasing amounts of HNE for 1 h. After 2 h, cells were harvested and lysed. Fifty μg of total protein was electrophoresed on a 10% SDS-PAGE gel, transferred to nitrocellulose, and probed with a polyclonal antibody specific to HNE-protein adducts at a dilution of 1:2500.

and p53 protein accumulation were detected in RAW parental cells within 3 h after exposure to 50 μM HNE (Fig. 4). Cytosolic cytrochrome *c* levels continued to increase through the 12 h after exposure, while p53 protein levels peaked at 6 h and decreased throughout the subsequent 6 h. Unlike parental cells, Bcl-2-expressing cells did not release any cytochrome *c* into the cytosol during the 12 h after exposure. However, these cells showed a slightly delayed increase in p53 protein that reached higher levels than in parental cells over the initial 12 h, and was sustained at these high levels for at least 96 h (Fig. 5).

The concentration dependence of HNE-induced cytochrome *c* release and p53 accumulation and their relationship to apoptosis were examined in more detail. When parental RAW 264.7 cells were exposed to 25–75 μM HNE, cytochrome *c* appeared in the cytosolic fraction at all concentrations within 6 h after the initial exposure. With increasing concentrations, a parallel increase in cytochrome *c* release was observed (Fig. 6). As previously observed at 50 μM HNE, Bcl-2-expressing cells showed no cytochrome *c* release throughout the range of HNE concentrations tested. Interestingly, p53 stabilization was not proportional to HNE concentration, and in fact p53 accumulation was more prominent at lower concentrations in RAW parental cells as well as the Bcl-2-expressing cells. It is possible that at concentrations as high as 75 μM, the protein kinases necessary for the phosphorylation and resulting stabilization of p53 are inhibited by HNE, albeit not completely in the Bcl-2-14 line. The DNA fragmentation assay showed apoptotic DNA fragmentation relatively early at 50 and 75 μM in RAW 264.7 parental cells. No detectable apoptosis occurred at any of the concentrations tested in Bcl-2-expressing cells (Fig. 7).

Effects of SV40 large T-antigen expression in HNE-treated RAW 264.7 cells

The role of p53 in HNE-induced apoptosis was further probed by expression of SV40 large T-antigen (TAg) in

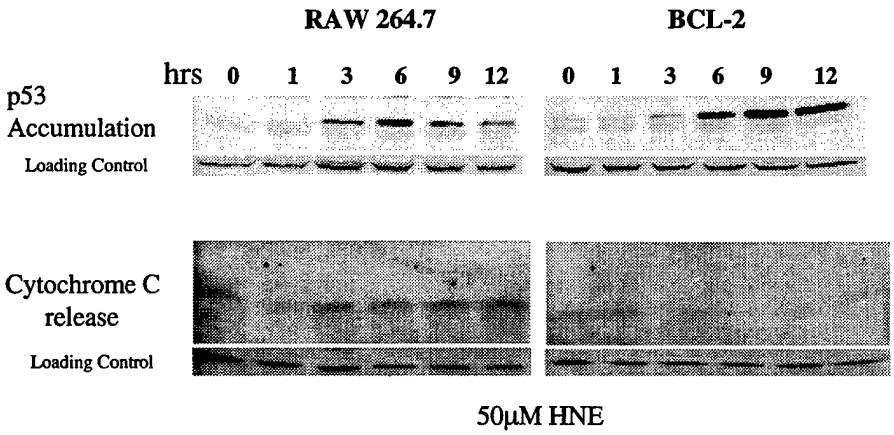

Fig. 4. HNE induces an accumulation of p53 protein in both parental and Bcl-2-expressing cells and a release of cytochrome *c* in parental cells. Bcl-2 protects against HNE-induced cytochrome *c* release. Cells were exposed to 50 μM HNE for 1 h in serum-free media. At the indicated times, cells were harvested and analyzed for either p53 stabilization or cytochrome *c* release. Total protein was electrophoresed on a 10% SDS-PAGE gel for p53 studies. P53 was probed with hybridoma supernatant pAB 122 [36] at a dilution of 1:100. For cytochrome *c* studies, cytosolic protein was isolated as described in Material and Methods, and 25 μg of protein was electrophoresed on a 15% SDS-PAGE gel and probed with 1 μg/ml anti-cytochrome *c* monoclonal antibody 7H8.2C12 (PharMingen; San Diego, CA, USA). Loading controls are shown to indicate equal protein loading.

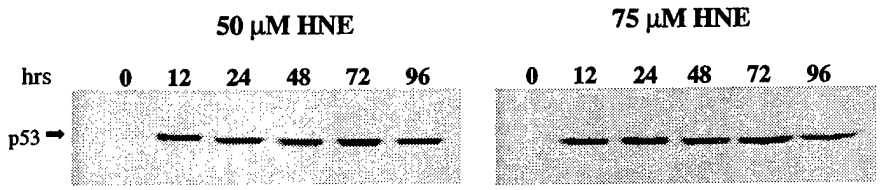

Fig. 5. HNE induces a sustained increase in p53 protein in Bcl-2-expressing cells. Bcl-2-expressing RAW 264.7 cells were harvested at the indicated times after a 1 h exposure to 50 μM HNE. Expression of p53 protein was measured by western blotting as described in the legend to Fig. 4.

RAW 264.7 parental cells by stable transfection. TAg is known to bind to p53 and interfere with its function by forming stable TAg-p53 complexes [28,29]. The effects of TAg expression on the levels of p53 and on the transactivation function of p53 was assessed by determining the levels of $p21^{WAF1/CIP1}$, a downstream effector known to be transcriptionally transactivated by p53. When exposed to HNE, control cells transfected with an empty vector exhibited a p53 accumulation pattern similar to that seen previously with parental cells (Fig. 8). Cells expressing TAg exhibited a substantial increase in p53 levels that was greater than that of empty vector control lines. There was also a general increase in the endogenous levels of p53 in the untreated TAg-expressing cells. This overall increase in p53 is likely due to the stabilization of p53 resulting from the formation of the TAg-p53 complex. While $p21^{WAF1/CIP1}$ levels increased substantially in control cells upon treatment with 30 or 50 μM HNE, this response was generally blocked in TAg-expressing cells. Only at 30 μM HNE, 6 h after exposure did $p21^{WAF1/CIP1}$ significantly increase. This brief increase, observed in all three experiments, may be due to transient excess of p53 relative to the amount of TAg present.

The effect of abrogation of p53 function by TAg on the apoptotic induction potential of HNE was assessed in control cells and TAg-expressing cells exposed to 30 or 50 μM HNE using DNA fragmentation as an index (Fig. 9). No discernible differences between control and TAg-expressing cells were detected, suggesting that the apoptotic potential of HNE is similar despite the changes in p53 levels and function due to TAg expression.

DISCUSSION

While much has been published on the cytotoxic effects of HNE, the discovery that HNE induces apoptosis is recent. The identification of HNE as an inducer of programmed cell death suggests a possible causative linkage between oxidant stress-induced lipid peroxidation and redox signaling or modulation of apoptosis. We have recently shown that while apoptosis can be caused by several lipid aldehydes produced by lipid peroxidation, HNE was the most potent inducer [12]. Therefore,

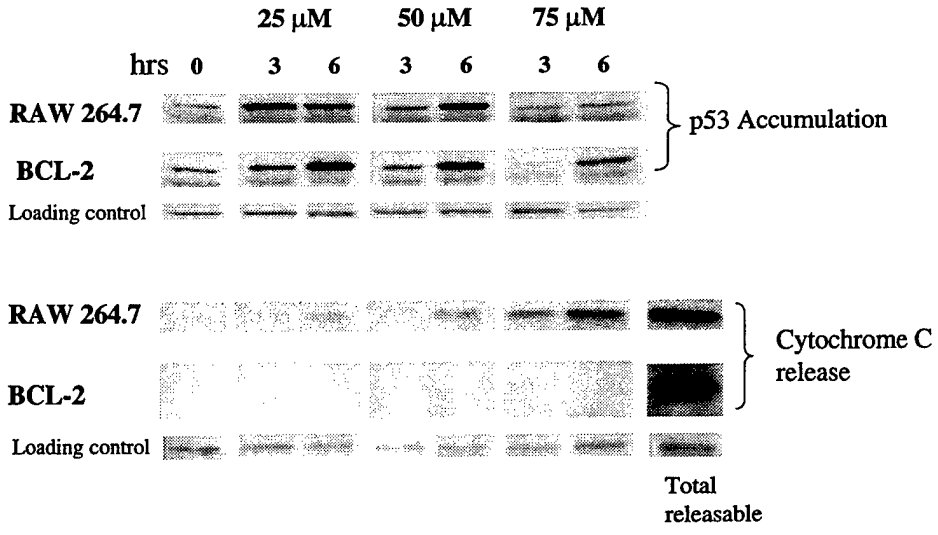

Fig. 6. Concentration-dependent patterns of p53 accumulation and cytochrome *c* release in both RAW 264.7 parental and Bcl-2 transfectants. Parental cells and Bcl-2 transfectant cells were exposed for 1 h to increasing concentrations of HNE, then analyzed for p53 or cytochrome *c* in cytosolic fractions as described in the legend to Fig. 4.

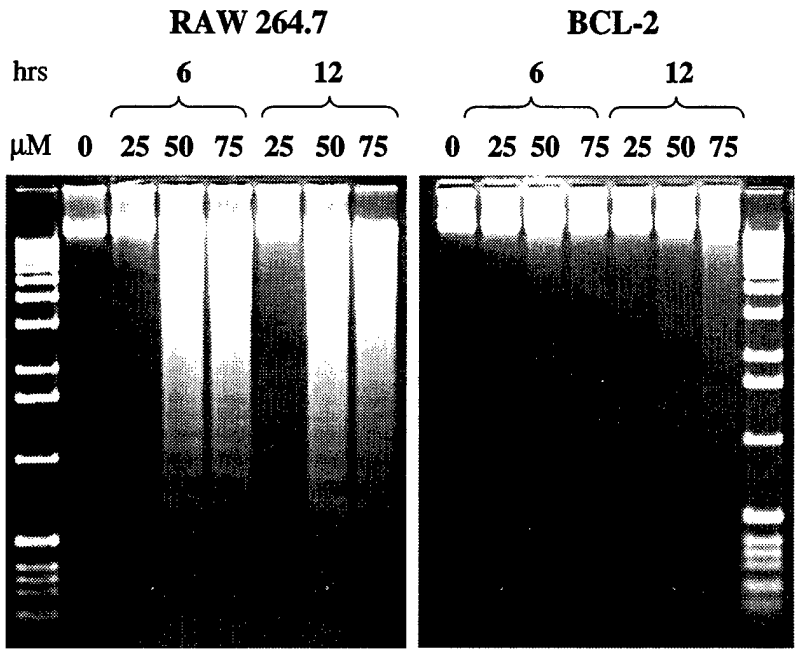

Fig. 7. Complete protection against HNE-induced apoptosis in RAW 264.7 cells overexpressing Bcl-2. Control cells and cells overexpressing Bcl-2 were exposed for 1 h in serum-free media containing increasing amounts of HNE. After 6 or 12 h, cells were harvested, lysed, and the DNA processed as described in Materials and Methods.

we examined mechanistic aspects of the cascade of events triggered by HNE that ultimately lead to the apoptotic death of the cell.

The high reactivity of HNE results in facile formation of Michael adducts with protein sulfhydryl-, amino-, and imidazole-functional groups of proteins [1]. Notably, several groups have reported damage by HNE to key enzymes in energy metabolism, and damage to mitochondrial proteins and function [1,40]. Chemical modification of DNA by in vitro exposure to HNE has been reported, and the resulting etheno-purine bases are elevated in relation to oxidative stress [41,42]. Clastogenic

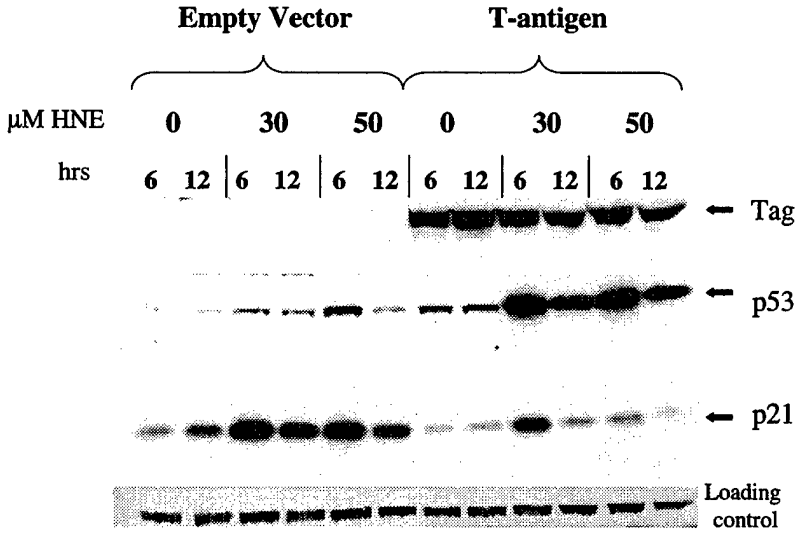

Fig. 8. Expression of SV40 large TAg resulted in an increase in endogenous p53, an increase in HNE-induced p53 accumulation, and a decrease in p53-mediated transactivation of $p21^{WAF1/CIP1}$. Control and TAg-expressing cells were exposed for 1 h to HNE. At the indicated times after the exposure, cells were harvested and lysed. Protein (100 μg/lane) was electrophoresed on a 10% SDS-PAGE gel, transferred to nitrocellulose, and TAg, p53, or $p21^{WAF1/CIP1}$ were detected by western blotting as described in Materials and Methods.

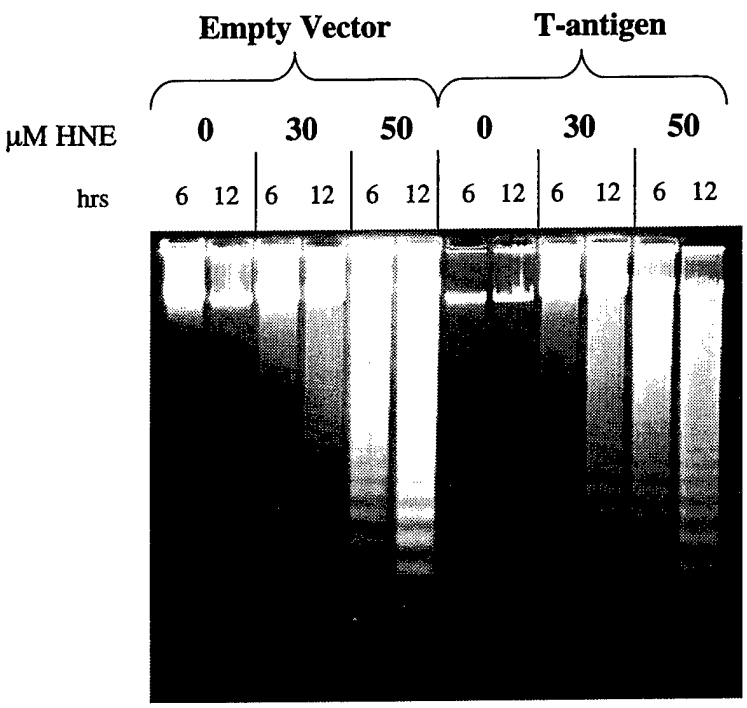

Fig. 9. Expression of TAg caused no significant difference in the levels of HNE-induced DNA fragmentation. Cells were exposed to 0, 30, or 50 μM HNE for 1 h in serum-free media and harvested and lysed at either 6 or 12 h later. DNA was isolated, precipitated, and processed as described in Materials and Methods.

and mutagenic effects by HNE including sister chromatid exchange and mutagenicity have also been reported [1,40]. These effects, and the previous finding that induction of apoptosis by nitric oxide is associated with p53 accumulation [34] suggested the possibility that p53 induction in response to DNA damage might play a role in HNE-induced apoptosis.

The potential roles of p53 induction and mitochondrial signaling were examined in the mouse macrophage cell line RAW 264.7, which is known to have wild-type, functional p53. Apoptosis was induced rapidly in a concentration-dependent manner in these cells with internucleosomal DNA fragmentation occurring as early as 6 h. However, overexpression of Bcl-2 protected the cells from loss of viability and induction of apoptosis throughout the range of HNE concentrations in which apoptosis is the primary mode of cell death. Expression of Bcl-2 is thought to protect cells at the level of the mitochondria primarily by preventing the release of cytochrome *c* into the cytosol [33]. This, together with the protective effect of Bcl-2 against HNE induction of apoptosis, further suggests a key role for mitochondria in HNE apoptotic signaling. Expression of Bcl-2 has also been shown to protect against oxidative stress, in some cases by enhancing GSH levels or preventing GSH depletion [43–45]. However, this does not appear to be a major factor in these studies, since we have found only moderate (< 30%) and transient (< 1 h) depletion of GSH by HNE under similar conditions (not shown). We have shown that while Bcl-2 protects against apoptosis, it does not protect against general HNE alkylation of protein. This suggests that Bcl-2 is protecting the cell downstream of the initial protein damage, which occurs equally in both parental and Bcl-2-expressing cells. Interestingly, in Bcl-2-expressing cells HNE caused a substantial growth delay of up to 48 h after exposure rather than cell death. This growth delay likely represents time required for the Bcl-2 cells to repair the cellular damage that would have induced apoptosis (as in the parental cell line) without the stabilizing downstream protection given by Bcl-2.

Apoptosis can occur as a result of DNA damage, a process mediated through the phosphorylation and subsequent stabilization and cellular accumulation of p53 protein [46]. Total cellular p53 levels increased significantly in HNE-treated cells over that of untreated controls, in parental cells, and to an even greater extent in Bcl-2 lines. Further p53 accumulation was transient in control cells while p53 levels remained elevated in Bcl-2-expressing cells for at least 96 h. Beyond the 48 h growth delay, Bcl-2 cells appear to grow normally with no apparent effect of the increased p53. This sustained level of p53 protein may be due to reduced turnover via protein degradation pathways. Indeed, a recent study showed that HNE covalently binds proteasomes and impairs ubiquitin/proteasomal-dependent proteolysis [9]. Modification of p53 by HNE may also prevent dephos-

phorylation or targeting for degradation by conjugation with ubiquitin.

Cytochrome *c* release occurred as early as 3 h after HNE exposure in parental cells, and increased with both time and HNE concentration. In contrast, Bcl-2 cells showed complete protection against cytochrome *c* release at all concentrations tested. The fact that Bcl-2 protected against apoptosis and protected against cytochrome *c* release suggests that HNE induces apoptotic cell death by a mechanism that is dependent on mitochondrial cytochrome *c* release. One possibilility is that HNE binds directly to a critical mitochondrial protein and induces a permeability transition that leads to cytochrome *c* release. For example, the adenine nucleotide transporter, which is thought to mediate the opening of the permeability transition pore that leads to the collapse of the transmembrane ionic potential, appears to contain a sensitive and accessible thiol group [47–49]. This possibility is particularly interesting because of the levels of lipid peroxidation and subsequent production of HNE that are produced directly in mitochondria due to the normal release of ROS within the mitochondria matrix resulting from oxidative metabolism.

The significance of p53 accumulation in HNE-induced apoptosis was further probed by using SV40 TAg expression as a means of blocking p53 protein function. Expression of TAg in RAW 264.7 cells did not alter morphology, growth rates, or basal levels of apoptosis. However, p53 function was blocked or reduced when compared to control, non-TAg-expressing cells. It is interesting to note that while levels of $p21^{WAF1/CIP1}$ are decreased, levels of p53 are significantly increased. This may be due to general stabilization of p53 in the TAg/p53 complex, which results in an overall increase in total p53 protein that is predominantly inactive.

Despite impairment of p53 transactivation due to complex formation with TAg, there was no change in HNE-induced apoptosis. Since neither HNE-induced p53 accumulation nor the TAg-mediated loss of p53 function had any effect on HNE-induced apoptosis, we conclude that p53 plays a minor, if any, role in HNE-induced apoptosis.

The mode of expression of apoptosis is known to vary considerably in different cell types even when triggered by the same insult, due to variations in the availability or sensitivity of specific regulatory pathways that are activated by a particular agent [50]. Hence, the importance of cytochrome *c* release in response to HNE may vary in other cell lines, due, for example, to differences in the number of mitochondria or to metabolism of HNE. Indeed, we have shown that expression of human aldehyde dehydrogenase-3 in RAW 264.1 greatly reduces HNE toxicity by converting HNE to 4-hydroxynonenoic acid, although the mode of death at the much higher concentrations required remains apoptotic [12]. The lack of a role of p53 in HNE-induced apoptosis was also examined in another cell line previously transfected with an inducible p53 expression vector [51]. Induction of p53 expression in H1299 lung cancer cells did not alter the kinetics or extent of HNE-induced apoptosis when compared to the p53-null parental cells (Haynes and Townsend, unpublished data). These results support our conclusion that p53 plays little or no role in the mechanism of induction of apoptosis by HNE.

In summary, we have shown that in RAW 264.7 mouse macrophages, HNE induces a cytochrome *c*-associated and apparently p53-independent apoptotic cell death. These findings contribute to what is known about the cellular effects of HNE, and provide evidence of a potential link between oxidant stress-induced lipid peroxidation and oxidant stress-induced apoptosis.

Acknowledgements — This work was supported by NIH Grant # RO1-CA-76283, DOD Breast Cancer Research Program Predoctoral Award #DAMD-17-98-1-8286, and Deutsche Forschungsgemeinschaft (Br 999), VerUm foundation, and utilized the Analytical Imaging and Tissue Culture Core facilities of the Comprehensive Cancer Center of Wake Forest University, supported by NIH Grant # P30-CA-12197-26.

REFERENCES

[1] Esterbauer, H.; Schaur, R. J.; Zollner, H. Chemistry and biochemistry of 4-hydroxynonenal, malonaldehyde and related aldehydes. *Free Radic. Biol. Med.* **11**:81–128; 1991.

[2] Witz, G. Biological interactions of α, β-unsaturated aldehydes. [Review] [114 refs]. *Free Radic. Biol. Med.* **7**:333–349; 1989.

[3] Cadenas, E.; Muller, A.; Brigelius, R.; Esterbauer, H.; Sies, H. Effects of 4-hydroxynonenal on isolated hepatocytes. *Biochem. J.* **214**:479–487; 1983.

[4] Poot, M.; Verkerk, A.; Koster, J.; Esterbauer, H.; Jongkind, J. Reversible inhibition of DNA and protein synthesis by cumene hydroperoxide and 4-hydroxy-nonenal. *Mech. Aging Dev.* **43**: 1–9; 1988.

[5] Benedetti, A.; Fulceri, R.; Comporti, M. Inhibition of calcium sequestration activity of liver microsomes by 4-hydroxyalkenals originating from the peroxidation of liver microsomal lipids. *Biochim. Biophys. Acta* **793**:489–493; 1984.

[6] Humphries, K. M.; Yoo, Y.; Szweda, L. I. Inhibition of NADH-linked mitochondrial respiration by 4-hydroxy-2-nonenal. *Biochemistry* **37**:552–557; 1998.

[7] Page, S.; Fischer, C.; Baumgartner, B.; Haas, M.; Kreusel, U.; Loidl, G.; Hayn, M.; Ziegler-Heitbrock, H. W. L.; Neumeier, D.; Brand, K. 4-Hydroxynonenal prevents NF-κB activation and tumor necrosis factor expression by inhibiting I κB phosphorylation and subsequent proteolysis. *J. Biol. Chem.* **274**:11611–11618; 1999.

[8] Soh, Y.; Jeong, K. S.; Lee, I. J.; Bae, M. A.; Kim, Y. C.; Song, B. J. Selective activation of the c-Jun N-terminal protein kinase pathway during 4-hydroxynonenal-induced apoptosis of PC12 cells. *Mol. Pharmacol.* **58**:535–541; 2000.

[9] Okada, K.; Wangpoengtrakul, C.; Osawa, T.; Toyokuni, S.; Tanaka, K.; Uchida, K. 4-Hydroxy-2-nonenal-mediated impairment of intracellular proteolysis during oxidative stress: identification of proteasomes as target molecules. *J. Biol. Chem.* **274**: 23787–23793; 1999.

[10] Kruman, I.; Bruce-Keller, A. J.; Bredesen, D.; Waeg, G.; Mattson, M. P. Evidence that 4-hydroxynonenal mediates oxidative stress-induced neuronal apoptosis. *J. Neurosci.* **17**:5089–5100; 1997.

[11] Li, L.; Hamilton, R. F. Jr.; Kirichenko, A.; Holian, A. 4-Hy-

droxynonenal-induced cell death in murine alveolar macrophages. *Toxicol. Appl. Pharmacol.* **139:**135–143; 1996.

[12] Haynes, R. L.; Szweda, L.; Pickin, K.; Welker, M. E.; Townsend, A. J. Structure-activity relationships for growth inhibition and induction of apoptosis by 4-hydroxy-2-nonenal in Raw 264.7 cells. *Mol. Pharmacol.* **58:**788–794; 2000.

[13] Sakamoto, A.; Ohnishi, S.; Ohnishi, T.; Ogawa, R. Relationship between free radical production and lipid peroxidation during ischemia-reperfusion injury in the rat brain. *Brain Res.* **554:**186–192; 1991.

[14] Maltzman, W.; Czyzyk, L. UV irradiation stimulates levels of p53 cellular tumor antigen in nontransformed mouse cells. *Molec. Cell. Biol.* **4:**1689–1694; 1984.

[15] Yamaizumi, M.; Sugano, T. UV-induced nuclear accumulation of p53 is evoked through DNA damage of actively transcribed genes independent of the cell cycle. *Oncogene* **9:**2775–2784; 1994.

[16] Kastan, M.; Onyekwere, O.; Sidransky, D.; Vogelstein, B.; Craig, R. Participation of p53 protein in the cellular response to DNA damage. *Cancer Res.* **51:**6304–6311; 1991.

[17] Kuerbitz, S.; Plunkett, B.; Walsh, W.; Kastan, M. Wild-type p53 is a cell cycle checkpoint determinant following irradiation. *Proc. Natl. Acad. Sci. USA* **89:**7491–7495; 1992.

[18] Zhan, Q.; Carrier, F.; Forance, A. Induction of cellular p53 activity by DNA-damaging agents and growth arrest. *Molec. Cell. Biol.* **13:**4242–4250; 1993.

[19] Tishler, R.; Calderwood, S.; Coleman, C.; Price, B. Increase in sequence-specific DNA binding by p53 following treatment with chemotherapeutic and DNA damaging agents. *Cancer Res.* **53:** 2212–2216; 1993.

[20] Shieh, S.; Ikeda, M.; Taya, Y.; Prives, C. DNA damage-induced phosphorylation of p53 alleviates inhibition by MDM2. *Cell* **91:**325–334; 1997.

[21] Siliciano, J.; Canman, C.; Taya, Y.; Sakaguchi, K.; Kastan, M. DNA damage induces phosphorylation of the amino terminus of P53. *Genes Devel.* **11:**3471–3481; 1997.

[22] Canman, C.; Lim, D.; Cimprich, K.; Taya, Y.; Tamai, K.; Sakaguchi, K.; Appella, E.; Kastan, M.; Siliciano, J. Activation of the ATM kinase by ionizing radiation and phosphorylation of p53. *Science* **281:**1677–1679; 1998.

[23] El-Deiry, W.; Tokino, T. V. V.; Levy, D.; Parsons, R.; Trent, J.; Lin, D.; Mercer, W.; Kinzler, K.; Vogelstein, B. Waf-1, a potential mediator of p53 tumor suppressor. *Cell* **75:**817–825; 1993.

[24] Miyashita, T.; Reed, J. Tumor suppressor p53 is a direct transactivational activator of the human bax gene. *Cell* **80:**293–299; 1995.

[25] Kastan, M.; Zhan, Q.; El-Deiry, W.; Carrier, F.; Jacks, T.; Walsh, W.; Plunkett, B.; Volgelstein, B.; Fornace, A. A mammalian cell cycle check point pathway utilizing p53 and GADD45 is defective in ataxia-telangiectasia. *Cell* **71:**587–597; 1992.

[26] Haupt, Y.; Maya, R.; Kazaz, A.; Oren, M. Mdm2 promotes the rapid degradation of p53. *Nature* **387:**296–298; 1997.

[27] Kupbutat, M.; Jones, S.; Vausder, K. Regulation of p53 stability by MDM2. *Nature* **387:**299–303; 1997.

[28] Zhu, J.; Abate, M.; Rice, P.; Cole, C. The ability of simian virus 40 large T-antigen to immortalize primary mouse embryo fibroblasts cosegregates with its ability to bind to p53. *J. Virol.* **65:**6872–6880; 1991.

[29] Mietz, J.; Unger, T.; Huibregatse, J.; Howley, P. The transcriptional transactivation function of WT p53 is inhibited by SV40 large T-antigen and by HPV-16 E6 oncoprotein. *EMBO J.* **11:** 5013–5020; 1992.

[30] Zamzami, N.; Marchetti, P.; Castedo, M.; Zanin, C.; Vayssiere, J.; Petit, P.; Kroemer, G. Reductions in mitochondrial potential constitutes an early irreversible step of programmed lymphocyte death in vivo. *J. Exper. Med.* **181:**1661–1672; 1995.

[31] Zamzami, N.; Marchetti, P.; Castedo, M.; Decaudin, D.; Macho, A.; Hirsch, T.; Susin, S.; Petit, P.; Mignotte, B.; Kroemer, G. Sequential reduction of mitochondrial transmembrane potential and generation of reactive oxygen species in early programmed cell death. *J. Exper. Med.* **182:**367–377; 1995.

[32] Liu, S.; Dixon, K. Induction of mutagenic DNA damage by chromium(VI) and glutathione. *Environ. Mol. Mutagen.* **28:**71–79; 1996.

[33] Tsujimo, Y.; Shimizu, S. BCL2 family: life or death switch. *FEBS Lett.* **466:**6–10; 2000.

[34] Messmer, U. K.; Reed, U. K.; Brune, B. Bcl-2 protects macrophages from nitric oxide-induced apoptosis. *J. Biol. Chem.* **271:** 20192–20197; 1996.

[35] Cohn, J. A.; Tsai, L.; Friguet, B.; Szweda, L. I. Chemical characterization of a protein-4-hydroxy-2-nonenal cross-link: immunochemical detection in mitochondria exposed to oxidative stress. *Arch. Biochem. Biophys.* **328:**158–164; 1996.

[36] Brockhaus, F.; Brune, B. P53 accumulation in apoptotic macrophages is an energy demanding process that preceeds cytochrome *c* release in response to nitric oxide. *Oncogene* **18:**6403–6410; 1999.

[37] Southern, P.; Berg, P. Transformation of mammalian cells to antibiotic resistancewith a bacterial gene under the control of the SV-40 early region promoter. *J. Molec. Appl. Genet.* **1:**327–341; 1982.

[38] Crawford, L.; Leppard, K.; Lane, D.; Harlow, E. Cellular proteins reactive with monoclonal antibodies directed against SV40 T-antigen. *J. Virol.* **42:**612–620; 1982.

[39] Brockhaus, F.; Brune, B. Overexpression of CuZn superoxide dismutase protects RAW 264.7 macrophages against nitric oxide cytotoxicity. *Biochem. J.* **338:**295–303; 1999.

[40] Esterbauer, H. Cytotoxicity and genotoxicity of lipid-oxidation products [Review]. *Am. J. Clin. Nutr.* **57:**779S–785S; 1993.

[41] Sodum, R. S.; Chung, F. L. 1,N2-ethenodeoxyguanosine as a potential marker for DNA adduct formation by trans-4-hydroxy-2-nonenal. *Canc. Res.* **48:**320–323; 1988.

[42] Winter, C. K.; Segall, H. J.; Haddon, W. F. Formation of cyclic adducts of deoxyguanosine with the aldehydes trans-4-hydroxy-2-hexenal and trans-4-hydroxy-2-nonenal in vitro. *Canc. Res.* **46:**5682–5686; 1986.

[43] Schor, N. F.; Rudin, C. M.; Hartman, A. R.; Thompson, C. B.; Tyurina, Y. Y.; Kagan, V. E. Cell line dependence of Bcl-2-induced alteration of glutathione handling. *Oncogene* **19:**472–476; 2000.

[44] Voehringer, D. W. Bcl-2 and glutathione: alterations in cellular redox state that regulate apoptosis sensitivity. *Free Radic. Biol. Med.* **27:**945–950; 1999.

[45] Xu, L. J.; Koumenis, I. L.; Tilly, J. L.; Giffard, R. G. Overexpression of Bcl-xL protects astrocyte from glucose deprivation and is associated with higher glutathione, ferritin, and iron levels. *Anesthesiology* **91:**1036–1046; 1999.

[46] Gottlieb, T.; Oren, M. P53 and apoptosis. *Semin. Canc. Biol.* **8:**359–368; 1998.

[47] Petronilli, V.; Costantini, P.; Scorrano, L.; Colonna, R.; Passamonti, S.; Bernardi, P. The voltage sensor of the mitochondrial permeability transition pore is tuned by the oxidation-reduction state of vicinal thiols. Increase of the gating potential by oxidants and its reversal by reducing agents. *J. Biol. Chem.* **269:**16638–16642; 1994.

[48] Costantini, P.; Chernyak, B.; Petronilli, V.; Bernardi, P. Modulation of the mitochondrial permeability transition pore by pyridine nucleotides and dithiol oxidation at two separate sites. *J. Biol. Chem.* **271:**6747–6751; 1996.

[49] Costantini, P.; Belzacq, A.; Vieiratt, L.; Larochette, N.; de Pablo, M.; Zamzami, N.; Susin, S. Oxidation of a critical thiol residue of the adenine nucleotide translocation enforces Bcl-2 independent permeability transition pore opening and apoptosis. *Oncogene* **19:** 307–314; 2000.

[50] Messmer, U. K.; Brune, B. Nitric oxide-induced apoptosis: p53-dependent and p53-independent signalling pathways. *Biochem. J.* **319:**299–305; 1996.

[51] Wang, Y.; Blandino, G.; Oren, M.; Givol, D. Induced p53 expression in a lung cancer cell line promotes cell senescence and differentially modifies the cytotoxicity of anti-cancer drugs. *Oncogene* **17:**1923–1930; 1998.

ABBREVIATIONS

DMEM—Dulbecco's minimal essential medium
EDTA—ethylene diamine tetraacetic acid
FBS—fetal bovine serum
GSH—glutathione
HNE—4-hydroxy-2-nonenal
NF-κB—nuclear factor κB
PBS—phosphate-buffered saline
PMSF—phenylmethylsulfonyl fluoride
ROS—reactive oxygen species
TAg—large T-antigen